



Disease-modifying treatment with I2 imidazoline receptor ligand LSL60101 in an Alzheimer's disease mouse model : A Comparative study with donepezil

| | |
|-------------------------------|--|
| Journal: | <i>British Journal of Pharmacology</i> |
| Manuscript ID | 2020-BJP-1766-RP.R1 |
| Manuscript Type: | Research Paper |
| Date Submitted by the Author: | n/a |
| Complete List of Authors: | Vasilopoulou, Fotini; Universitat de Barcelona Facultat de Farmacia, Pharmacology, Toxicology and Therapeutic Chemistry Rodríguez-Arevalo, Sergio; Universitat de Barcelona Facultat de Farmacia, Pharmacology, Toxicology and Therapeutic Chemistry Bagán, Andrea; Universitat de Barcelona Facultat de Farmacia, Pharmacology, Toxicology and Therapeutic Chemistry Escolano, Carmen; Universitat de Barcelona Facultat de Farmacia, Pharmacology, Toxicology and Therapeutic Chemistry Griñán-Ferré, Christian; Universitat de Barcelona Facultat de Farmacia, Pharmacology, Toxicology and Therapeutic Chemistry Pallàs, Mercè; Universitat de Barcelona Facultat de Farmacia, Pharmacology, Toxicology and Therapeutic Chemistry |
| Major area of pharmacology: | Neuropharmacology, Neurodegeneration/neuroprotection |
| Cross-cutting area: | Drug discovery/target validation, Biochemical pharmacology |
| Additional area(s): | Ageing/aging, Ligands, In vivo, Glia |
| | |

SCHOLARONE™
Manuscripts

Disease-modifying treatment with I2 imidazoline receptor ligand LSL60101 in an Alzheimer's disease mouse model: A Comparative study with donepezil.

Running Title: I2 Imidazoline receptor modulation as a potential therapeutic strategy against Alzheimer's Disease.

Foteini Vasilopoulou¹, Sergio Rodríguez-Arévalo², Andrea Bagán², Carmen Escolano², Christian Griñán-Ferré^{1*} and Mercè Pallàs^{1*}

¹Pharmacology Section. Department of Pharmacology, Toxicology and Medicinal Chemistry, Faculty of Pharmacy and Food Sciences, and Institut de Neurociències, University of Barcelona, Av. Joan XXIII, 27-31, E-08028 Barcelona, Spain.

²Laboratory of Medicinal Chemistry (Associated Unit to CSIC), Department of Pharmacology, Toxicology and Medicinal Chemistry, Faculty of Pharmacy and Food Sciences, and Institute of Biomedicine (IBUB), University of Barcelona, Av. Joan XXIII, 27-31, E-08028 Barcelona, Spain.

***Corresponding authors**

WORD COUNT: Main text 6359 words (Introduction, methods, results and discussion) and 3317 words (excluding methods, references and figure legends)

ACKNOWLEDGEMENTS

This study was supported by Ministerio de Economía y Competitividad of Spain and FEDER (PID2019-107991RB-I00, PID2019-106285RB-I00) and 2017SGR106 (AGAUR, Catalonia). The project leading to these results has received funding from "la Caixa" Foundation (ID100010434), under agreement CI18-00002. F.V. thanks the UB for the APIF grant (UB2016); S. R.-A. to Generalitat de Catalunya, (2018FI-B-00227), and A. B. for the APIF Grant Institute of Biomedicine (UB2018).

AUTHOR CONTRIBUTIONS

FV, CG-F and MP conceived the study, designed all the experiments, and interpreted the data; FV, CG-F performed the experiments and data analysis; all authors revised the manuscript

draft. S R-A, AB and CE synthesised compounds tested; FV, CG-F and MP wrote, revised, and finalised the manuscript.

CONFLICT OF INTEREST

The authors declare no conflicts of interest.

DECLARATION OF TRANSPARENCY AND SCIENTIFIC RIGOUR

This Declaration acknowledges that this paper adheres to the principles for transparent reporting and scientific rigour of preclinical research as stated in the *BJP* guidelines for [Design & Analysis](#), [Immunoblotting and Immunochemistry](#) and [Animal Experimentation](#) and as recommended by funding agencies, publishers and other organizations engaged with supporting research.

DATA AVAILABILITY STATEMENT

The data that support the findings of this study are available from the corresponding author upon reasonable request. Some data may not be available because of privacy or ethical restrictions.

ABSTRACT

Background and Purpose: The development of effective therapeutic strategies against Alzheimer's disease (AD) remains a challenge. I2 Imidazoline receptors (I2-IR) ligands have a neuroprotective role in AD. Moreover, co-treatment of acetylcholinesterase inhibitors with neuroprotective agents has shown better effects on the prevention of dementia. Here, we assessed the potential therapeutic effect of the I2-IR ligand LSL60101, donepezil, and their combination in 5XFAD mice.

Experimental Approach: 5XFAD female mice were treated with low doses of LSL60101 (1 mg kg⁻¹ day⁻¹), donepezil (1 mg kg⁻¹ day⁻¹), and donepezil plus LSL60101 (1+1 mg kg⁻¹ day⁻¹), during 4 weeks *per os*. Novel object recognition, Morris water maze, open field, elevated plus maze, and three-chamber tests were employed to evaluate the cognitive and behavioural status after treatment. The effects of the treatments on AD-like pathology were assessed with immunohistochemistry, Western blot and qPCR.

Key results: Chronic low-dose treatment with LSL60101 and donepezil reversed cognitive deficits and impaired social behaviour. LSL60101 treatment did not affect anxiety-like behaviour in contrast to donepezil. In the 5XFAD brains, LSL60101 and donepezil/LSL60101 treatments decreased A β -pathology and Tau hyperphosphorylation, and these alterations were accompanied by reduced microglia marker Iba-1 levels and increased *Trem2* gene expression. LSL60601 and donepezil decreased glial fibrillary acidic protein (GFAP) astrocytic marker reactivity. However, only LSL60601 treatment significantly increased the synaptic markers' levels post-density 95 (PSD95) and synaptophysin (SYN).

Conclusion and implications: Our results suggest that chronic low dose treatment with selective I2-IR ligands can be an effective treatment for AD and provide insights into combination treatments of symptomatic and disease-modifying drugs.

KEYWORDS: I2 Imidazoline receptors, β -amyloid, neuroinflammation, synaptic plasticity, donepezil, Alzheimer's disease

BULLET POINT SUMMARY

What is already known

- I2-IR modulation by selective I2-IR ligands delivers neuroprotection in the central nervous system.
- AchEI do not modify disease progression; thereby, a new drug for halting AD progression is needed.

What this study adds

- LSL60101, an I2-IR ligand, treatment rescued 5XFAD mice from cognitive impairments and modified disease progression.
- LSL60101 treatment provides greater effects on AD-hallmarks and synaptic plasticity than donepezil, even in combination.

Clinical significance

- Chronic treatment with I2-IR ligands would constitute a relevant therapeutic disease-modifying strategy against AD.

1. INTRODUCTION

Alzheimer's disease (AD) is the leading cause of dementia among the elderly and the most common irreversible and incurable neurodegenerative disorder, clinically characterised by progressive behavioural disturbances and memory loss (Murray et al., 2011). Amyloid β (A β) plaques and neurofibrillary tangles, consisting of hyperphosphorylated Tau (p-Tau), are two major neuropathological AD hallmarks, which lead to synaptic failure (Walsh and Selkoe, 2004; Selkoe, 2008; DeTure and Dickson, 2019). Moreover, the inflammatory response triggered by A β deposits and Tau hyperphosphorylation, among others and mediated by activated microglia and reactive astrocytes, has a key role in the progression of AD (Dickson and Rogers, 1992; MERAZ RIOS et al., 2013). Thus, targeting A β aggregation, p-Tau, and neuroinflammation has been proved so far, the main disease-modifying strategy for treating AD.

However, up to date, only symptomatic treatments, including the acetylcholinesterase inhibitors (AChEI) and the [N-methyl-D-aspartate](#) (NMDAr) antagonists, are available for AD therapy. Those drugs showed modest symptomatic benefits on behaviour and cognition, but they did not halt its progression (Grossberg, 2003; Mehta et al., 2012). Among AChEI, donepezil is clinically used for cognitive dysfunction in AD (Giacobini, 2000). Besides its main effects related to the enhancement of cholinergic transmission, donepezil has been demonstrated to exert the potential for disease pathway modifications in AD, including attenuation of A β load and anti-inflammatory properties *in vitro* and *in vivo* (Kim et al., 2014). However, at a clinical level, it lacks a curative effect; thereby, identifying new molecular targets for the development of treatments is crucial. In this context, to further enhance the non-cholinergic therapeutic effects of donepezil, a combination of donepezil with other neuroprotective agents could provide a novel approach to preserve cognitive function and/or delay AD pathology.

I2 imidazoline receptors (I2-IR) are receiving growing attention due to the neuroprotective effects in the central nervous system (CNS) (Bousquet et al., 2020). In the brain, I2-IR are

found in both neurons and glial cells (Regunathan et al., 1993; Olmos et al., 1994), and their modulation has been associated with neurodegenerative disorders, including AD (Ruiz et al., 1993). Most notably, the density of I2-IR was found to increase in AD patients (Garcia-Sevilla et al., 1998). Several lines of evidence provided by our group demonstrated that selective I2-IR ligands protected against cognitive impairment ameliorating AD pathological features related to APP processing, Tau hyperphosphorylation, neuroinflammation, and oxidative stress (OS) processes, using well-established AD animal models (Abás et al., 2017, 2020; Griñán-Ferré et al., 2019; Vasilopoulou et al., 2020b). Likewise, [agmatine](#), the proposed endogenous ligand for I2-IR, prevented cognitive deficits in A β 1-42 peptide injected mice, and of note, its effect was augmented and attenuated by I2-IR agonists and antagonists, respectively (Kotagale et al., 2020). Collectively, this evidence supports the potential therapeutic effect of I2-IR ligands in AD.

Among the I2-IR ligands, the selective I2-IR ligand LSL60101 [2-(2-benzofuranyl)imidazole]] (Ki ratio for α_2 /I2-receptors=286) has been associated with the induction of several central effects, such as acute hyperphagic effects (Menargues et al., 1994) and inhibition of the development of opioid-induced tolerance and potentiation of morphine analgesia (Boronat et al., 1998). Interestingly, LSL60101 was shown to promote neuronal protection mediated by the induction of reactive astrocytes (Casanovas et al., 2000). However, the neuroprotective effect of LSL60101 on AD pathological conditions has not been reported.

Taking into account that women have a higher risk of dementia and females are underrepresented in rodent models of AD, in the present *in vivo* study, we explored the I2-IR ligand LSL60101 beneficial effects on the behavioural capabilities and cognitive impairments presented in AD, as well as on AD hallmarks, including neuroinflammation, glial reactivity, and synaptic plasticity, by using 5XFAD females, a widely accepted transgenic mouse model for early-onset AD. Additionally, the comparative effect with donepezil, considered a symptomatic AD treatment, was investigated alone and in combination therapy with the I2-IR ligand LSL60101 to decipher joint effects of both compounds in ameliorating AD pathology and molecular changes presented by 5XFAD mice.

2. METHODS

2.1 Animals

The 5XFAD mouse model is a well-characterised double transgenic APP/PSEN1 model, which co-expressed 5 familial AD mutations. This animal model incorporates AD pathological characteristics, including early plaque formation and gliosis starting at 2 months, robust cognitive and behavioural deficits such as memory impairment, reduced anxiety and social disturbances starting at 4-5 months, and neuronal loss at 6 months. (Oakley et al., 2006; Landel et al., 2014; Griñán-Ferré et al., 2018). Thus, at the selected age of 7 months, 5XFAD mice provide a severe AD pathological landscape suitable for evaluating the drug effects.

In the present study, 5XFAD (n = 47) and Wild-Type (WT, n = 46) female mice (7-month-old) were used to perform behavioural and molecular analyses. Females were used because AD incidence is higher in women and few studies are available. WT animals were randomly divided into WT Control (**WT Ct**) (n=11), WT treated with donepezil ($1 \text{ mg}^{-1} \text{ kg}^{-1} \text{ day}^{-1}$) (**WT Dp**) (n=12), LSL60101 (**WT LSL**) ($1 \text{ mg}^{-1} \text{ kg}^{-1} \text{ day}^{-1}$) (n=12), and the co-treatment donepezil ($1 \text{ mg}^{-1} \text{ kg}^{-1} \text{ day}^{-1}$) and LSL60101 ($1 \text{ mg}^{-1} \text{ kg}^{-1} \text{ day}^{-1}$) (**WT Dp+LSL**). 5XFAD mice were randomly divided into: 5XFAD Control (**5XFAD Ct**) (n=11), 5XFAD treated with Donepezil ($1 \text{ mg}^{-1} \text{ kg}^{-1} \text{ day}^{-1}$) (**5XFAD Dp**) (n=12), LSL60101 (**5XFAD LSL**) ($1 \text{ mg}^{-1} \text{ kg}^{-1} \text{ day}^{-1}$) (n=12), and the co-treatment Donepezil ($1 \text{ mg}^{-1} \text{ kg}^{-1} \text{ day}^{-1}$) and LSL60101 ($1 \text{ mg}^{-1} \text{ kg}^{-1} \text{ day}^{-1}$) (**5XFAD Dp+LSL**).

The animals had free access to food and water and were kept under standard temperature conditions ($22 \pm 2^\circ\text{C}$) and 12-h/12-h light/dark cycles (300 lux/0 lux). Compounds were dissolved in 1.8% (2-hydroxypropyl)- β -cyclodextrin and administered through drinking water. Control groups received water plus 1.8% (2-hydroxypropyl)- β -cyclodextrin during the treatment period. For the drugs' administration, dosages were calculated based on average daily water consumption recorded in each cage, and they were confirmed by re-calculations once a week. Each animal's weight was also recorded once a week during the treatment period, and the drug dosages were recalculated when necessary based on the results. The average daily water consumption was 5 mL/day for each animal without observing significant differences among the groups. Likewise, the bodyweight of the control and treated groups did not change significantly during the treatment period (Supplementary Figure S1). The intervention sample size was chosen following previous studies in our laboratory and using one of the available interactive tools (<http://www.biomath.info/power/index.html>). Moreover, the animal number mismatch among experimental groups was due to the

exclusion of mice by death or ethical reasons according to the final point indicated in the approved protocol.

After 4 weeks of treatment, behavioural and cognitive tests were performed to study the effects of treatment on learning, memory, anxiety behaviour, and social interaction (Fig. 1a); during this period and up to the euthanasia. All studies and procedures for the mouse behaviour tests, brain dissection, and extractions followed the ARRIVE (Lilley et al., 2020) and standard ethical guidelines (European Communities Council Directive 2010/63/EU and Guidelines for the Care and Use of Mammals in Neuroscience and Behavioural Research, National Research Council 2003) and were approved by Bioethical Committees from the University of Barcelona and the Government of Catalonia.

2.2 Behavioural tests

2.2.1 Novel Object Recognition Test (NORT)

A modification of the NORT protocol was performed (Ennaceur and Delacour, 1988). In brief, mice were placed in a 90° two-arm (25 x 20 x 5 cm) black maze, with removable walls for easy cleaning, and light intensity in mid-field was 30 lux. Before the memory trials mice were habituated to the apparatus for 10 min for 3 days. On day 4, the animals were submitted to a 10 min acquisition trial, in which they were allowed to freely explore two identical objects located at the end of each arm (First trial-Familiarization). After 2h (for short-term memory evaluation) and 24h (for long-term memory evaluation) from the first trial, the mice were submitted to a 10 min retention trial, in which one of the two identical objects had been replaced by a novel one. The behaviour was recorded, and the time that the mice spent exploring the new object (TN) and the old one (TO) were measured manually. Exploration was defined as sniffing or touching the objects with nose and/or forepaws. The discrimination index (DI) was calculated as $(TN-TO)/(TN+TO)$. To avoid object preference biases, objects were alternated. 70% EtOH was used to clean the arms and objects after each trial to eliminate olfactory cues.

2.2.2 Morris Water Maze (MWM)

The MWM test was performed as described previously (Griñan-Ferré et al., 2016) in an open circular pool, filled with water which temperature was maintained at $22\text{ }^{\circ}\text{C} \pm 1$. The water surface was divided into four quadrants (Q1, Q2, Q3, and Q4) by two principal perpendicular axes, and five starting points were set (1,2,3,4). Four visual clues were placed on the walls of the tank (1,2,3,4). The animals' swimming paths were recorded, and the data were analysed with SMART version 3.0 software. On day 1, mice were placed individually into the pool, facing the wall, and allowed to swim for 60 seconds to be habituated to the experimental conditions. On day 2, a white platform was submerged 1.5 cm below the water level in the middle of the Q1 platform, and the acquisition phase took place for 5 days. Each day the animals were submitted to five trials starting from the positions set in random order. At each trial, mice were allowed to swim for 60 seconds and, if not able to find the platform within 60 seconds, were guided to the visible platform. The mice remained for 30s onto the platform for spatial orientation. There was no resting phase between each trial and the subsequent one. 24h after the last training, a memory test was performed. For this, the platform was removed from the pool and the mice were tested for 60s. The distance to the target, and the time spent in the platform quadrant (Q1), among other parameters, were measured.

2.2.3 Open Field (OF)

Emotional alterations and locomotor activity were evaluated by the OF test using a white plywood apparatus ($50 \times 50 \times 25$ cm) as previously described (Archer, 1973; Griñan-Ferré et al., 2016). The apparatus's ground was divided into the centre and peripheral area. Each individual was placed at the centre of the open field and allowed to explore the apparatus for 5 min. The apparatus was cleaned with 70% ethanol after between trials. The behaviour was recorded and later analysed with SMART ver. 3.0 software (Panlab). The locomotor activity of the mice calculated as the sum of total distance travelled in 5 min, the centre stay duration, and the number of rearings were evaluated.

2.2.4 Elevated Plus Maze (EPM)

Animals were tested for anxiety-like behaviour by performing the EPM test, based on a previously described protocol (Walf and Frye, 2007). The EPM apparatus consisted of two open arms ($30 \times 5 \times 15$ cm) and two closed arms ($30 \times 5 \times 15$ cm). The mice were placed at the

arms' junction and allowed to explore the apparatus for 5 min freely. EPM apparatus was cleaned with 70% ethanol between tests. The behaviour was recorded and later analysed with SMART ver. 3.0 software (Panlab). Parameters recorded included the total distance travelled during the 5 min test, the time spent in open arms, closed arms, and centre, as well as the number of rearings.

2.2.5 Three-Chamber Test (TCT)

Social behaviour of the mice was evaluated by the TCT following a previously described protocol (Companys-Alemany et al., 2020). A box (15x15x20 cm) divided into three equally dimensioned rooms with openings among them was used. The mice were submitted to 15-min trials. First, each mouse was placed in the centre of the box and allowed to explore the three chambers for 5 min (habituation). The entries to each room were measured manually. Afterwards, an intruder (same-sex and age) was placed in a metal cage in one of the rooms, and behaviour was recorded for 10 min. The time spent in each room and interacting with the intruder (e.g., sniffing, grooming) were measured manually. The TCT apparatus was cleaned with 70% ethanol between the trials to eliminate olfactory cues.

2.3 Brain processing

Mice were euthanised by cervical dislocation 3 days after the behavioural and cognitive tests were completed. The brains were immediately removed from the skulls, and the hippocampi were dissected, frozen and maintained at -80°C . For immunohistochemistry (IHC) experiments, mice were anaesthetised (ketamine $100\text{ mg}^{-1}\text{ kg}^{-1}$ and xylazine $10\text{ mg}^{-1}\text{ kg}^{-1}$), intraperitoneally and then perfused with 4% paraformaldehyde (PFA) diluted in 0.1 M phosphate buffer solution intracardially. Their brains were removed and postfixed in 4% PFA overnight at 4°C . Afterwards, the solutions were changed to PFA + 15% sucrose. Finally, the brains were frozen on powdered dry ice and stored at -80°C until sectioning.

2.4 Protein levels determination by Western blotting

For protein extraction, hippocampus samples were thawed and mixed in 200 μL lysis buffer (50 mM Tris-HCl pH 7.4, 150 mM NaCl, 5mM EDTA, 1% Triton X-100) containing phosphatase

and protease inhibitor cocktail (Cocktail II, Sigma-Aldrich). Once homogenised, samples were maintained on ice for 30 min. Afterwards, the samples were centrifuged at 10,000x g for 30 min at 4 °C, and the supernatants were collected and maintained at -80 °C. Total protein amount was quantified with the method of Bradford as described previously (Bradford, 1976).

For WB, aliquots of 15 µg of hippocampal protein were used. Protein samples were separated by Sodium dodecyl sulphate-Polyacrylamide gel electrophoresis (SDS-PAGE) (8-16%) and transferred onto Polyvinylidene difluoride (PVDF) membranes (Millipore). Afterwards, membranes were blocked in 5% bovine serum albumin (BSA) in 0,1% Tris-buffered saline - Tween20 (TBS-T) for 1h at room temperature, followed by overnight incubation at 4°C with the primary antibodies listed in Supplementary Table S1. Membranes were washed and incubated with secondary antibodies for 1h at room temperature. Immunoreactive proteins were viewed with a chemiluminescence-based detection kit, following the manufacturer's protocol (ECL Kit; Millipore), and digital images were acquired using a ChemiDoc XRS+ System (BioRad). Semi-quantitative analyses were carried out using ImageLab software (BioRad), and results were expressed in Arbitrary Units (AU), considering control protein levels as 100%. Protein loading was routinely monitored by immunodetection of glyceraldehyde-3-phosphate dehydrogenase (GADPH) or β-actin.

2.5 RNA extraction and gene expression determination

Total RNA isolation from hippocampal samples was performed using the TRIzol® reagent according to the manufacturer's instructions (Bioline Reagent). The yield, purity, and quality of RNA were determined spectrophotometrically with a NanoDrop™ND-1000 apparatus (Thermo Scientific) and an Agilent 2100B Bioanalyzer (Agilent Technologies). RNA samples with 260/280 ratios and RINs higher than 1.9 and 7.5, respectively, were selected. Reverse Transcription-Polymerase Chain Reaction (RT-PCR) was performed. Briefly, 2 µg of messenger RNA (mRNA) was reverse transcribed using a high-capacity cDNA reverse transcription kit (Applied Biosystems).

SYBR® Green real-time PCR was performed using a Step One Plus Detection System (Applied-Biosystems) with SYBR® Green PCR Master Mix (Applied-Biosystems). Each reaction mixture contained 6.75 µL of complementary DNA (cDNA) (with a concentration of 2µg), 0.75 µL of

each primer (with a concentration of 100nM), and 6.75 μ L of SYBR[®] Green PCR Master Mix (2x).

The data were analysed utilising the comparative cycle threshold (Ct) ($\Delta\Delta$ Ct) method, in which the levels of a housekeeping gene are used to normalise differences in sample loading and preparation. The normalisation of expression levels was performed with β -actin. The primer sequences and TaqMan probes used in this study are presented in Supplementary Table S2. Each sample was analysed in duplicate, and the results represent the n-fold difference in the transcript levels among different groups.

2.6. Glial immunohistochemical identification

For immunohistochemical studies, the frozen brains were embedded in OCT Cryostat Embedding Compound (Tissue-Tek, Torrance, Ca, USA), and 30- μ m-thick brain coronal sections were obtained at -20 °C on a cryostat (Leica Microsystems CM 3050S cryostat, Wetzlar, Germany), and kept in a cryoprotectant solution at -20°C until use. Free-floating slices were placed in a 24-well plate and washed with 0.01M PBS. Next, the free-floating sections were blocked with 0.1M PBS solution containing 1% BSA, 0,3% Triton X-100 for 20min at room temperature. Afterwards, slices were washed with PBS 0.01M two times for 5 min each and were incubated with the primary antibodies listed in Table X overnight at 4°C. The primary antibodies were diluted in a 0.1M PBS solution containing 1% BSA and 0.3% Triton x-100. On the following day, the coronal slices were washed with 0.1M PBS 0.1M 2 times for 5 min each and then incubated with the secondary antibodies listed in Supplementary Table S1 at room temperature for 1h. Later, the sections were washed 2 times for 5 min each with 0.1M PBS and were incubated with 5 μ M Hoechst staining solution (Sigma-Aldrich, St. Louis, MO) for 5 min in the dark at room temperature. After being washed, the slices were mounted using Fluoromount-G (EMS, USA).

2.7. Amyloid β plaques histology

A β plaques were stained with Thioflavin-S. Brain coronal sections of 30 μ m were obtained (Leica Microsystems CM 3050S cryostat, Wetzlar, Germany) and kept in a cryoprotectant solution at -20°C until use. Free-floating slices were placed in a 24-well plate and washed with 0.01M PBS for 5 min at room temperature to be rehydrated. Next, the brain sections were washed with 70% ethanol for 1 min, followed by a wash with 80% ethanol for 1 min. The slices

were then incubated with 0.3% Thioflavin-S (Sigma-Aldrich) solution for 15 min at room temperature in the dark. Afterwards, the samples were washed using 80%, 70%, and 50% EtOH for 1 min. Three 2-min washes with 0.1M PBS and the slices were mounted using Fluoromount-G (EMS, USA).

2.8 Image acquisition and analysis

Image acquisition was performed with a fluorescence laser microscope (Olympus BX51, Germany) using 4X, 10X, 20X objectives, and images were analysed using Image J software as previously described. For quantification of amyloid plaques, similar and comparable histological areas were selected, focusing on the adjacent positioning of the whole cortical area and the hippocampus of the one brain hemisphere. The images were converted to 8-bit grayscale images, thresholded within the linear range and the number of particles (Analyse particle function 10-Infinity), as well as the percentage of area covered by Thioflavin-S (20X objective), was calculated and averaged from two different sections from each animal. Glial fibrillary acidic protein (GFAP) and Iba-1 stained images (10X objective) were acquired, maintaining constant exposure for all samples across single experiments. The fluorescence intensity of the positive cells was measured in hippocampal CA1, CA3, and Dentate gyrus (DG) areas, and quantification was averaged from two to three different sections from each animal.

2.9 Statistical Analysis

The data and statistical analysis comply with British Journal of Pharmacology's recommendations on experimental design and analysis in pharmacology (Curtis et al., 2018). Group size may vary according to power analysis and expertise of the authors regarding the behavioural tests (Griñan-Ferré et al., 2016; Griñan-Ferré et al., 2018), and statistical analysis was undertaken only for studies where each group size was at least $n=5$. The blinded analysis was performed for behavioural tests. All data are expressed as the mean \pm standard error of the mean (SEM). Statistical analysis was conducted using GraphPad Prism version 8 statistical software. All data were tested for normal distribution and equal variance. In the cognitive and behavioural studies, means were compared with two-way ANOVA or one-way ANOVA when necessary, followed by Tukey's post hoc tests. In molecular studies, means were compared with two-tailed unpaired Student's t-test (WT Control vs 5XFAD Control) or one-way ANOVA followed by Tukey's post hoc tests (5XFAD Control vs 5XFAD treated groups). Statistical

significance was considered when P values were <0.05 . Statistical outliers were determined with Grubbs' test and, when necessary, were removed.

2.10 Nomenclature of Targets and Ligands

Key protein targets and ligands in this article are hyperlinked to corresponding entries in <http://www.guidetopharmacology.org>, the common portal for data from the IUPHAR/BPS Guide to PHARMACOLOGY and are permanently archived in the Concise Guide to PHARMACOLOGY 2019/20.

RESULTS

3.1 I2-IR ligand LSL60101 and donepezil improve memory deficits in 5XFAD mice.

Short- and long-term working memory were evaluated by NORT. 7-month-old 5XFAD mice presented robust cognitive deficits compared to WT (Figures 1b, 1c). LSL60101 treatment resulted in a rapid and sustained recovery of cognitive function by increasing the DI in both 2h and 24h memory tests (Figures 1b, 1c). Donepezil enhanced but did not sustain memory function in 5XFAD mice, as a significant increase of the DI was found after 2h, but not at 24h memory test (Figures 1b, 1c). Co-treatment did not improve cognition in comparison with individual treatments (Figures 1b, 1c). Treatments had no significant effects on WT's cognitive performance (Figures 1b, 1c).

For spatial learning and memory evaluation, the MWM was performed. After 5 days of training, all experimental groups presented curves with progressively shorter path length on consecutive days. Of note, the path length to the platform was significantly decreased in LSL60101 treated 5XFAD mice when compared to 5XFAD controls (Figure 1d). In the probe trial, 5XFAD mice showed a reduced percentage of time spent in the platform quadrant while the mice spent significantly more time in the quadrant opposite to the platform. Moreover, 5XFAD control mice presented increased latency to target compared to WT mice, and in whole, a weaker cognitive performance. (Figure 1e, 1h, 1g, Supplementary Figure S2). LSL60101 treatment significantly increased the time spent in the platform quadrant in the 5XFAD treated mice compared to both vehicle and donepezil treated 5XFAD, whereas LSL60101 treatment had no effect on WT's (Figures 1e, 1f, 1h). Neither donepezil nor co-

treatment improved 5XFAD mice spatial memory (Figures 1d, 1e). Although WT treated mice performed better (Figures 1d, 1f, 1h). All treatments decreased the path length to the platform, albeit not significantly, due to the different performance of individual mice (Supplementary Figure S2).

3.2 I2-IR ligand LSL60101 does not affect behavioural and emotional disturbances in 5XFAD mice in contrast to donepezil.

We also investigated the effect of the treatments on the 5XFAD and WT mice anxiety-like behaviour by performing the OF and EPM tests. No differences in locomotor activity were observed among the WT and 5XFAD groups (Figure 2a). 5XFAD mice presented a significant increase in the time spent in the centre of the open field compared to WT mice (Figure 2b). No effect was observed on the WT mice behaviour after treatments. 5XFAD treated with donepezil but not with LSL60101 showed a significant decrease in the time spent in the centre compared to 5XFAD controls, reverting to the WT healthy phenotype (Figure 2b). Co-treatment LSL60101/donepezil displayed the same results that showed donepezil alone in all parameters evaluated (Figure 2b and Supplementary Table S3).

Similarly, in the EPM, 5XFAD mice spent significantly more time in the open arms and less in the closed arms in comparison with age-matched WTs (Figures 2d, 2e). Donepezil had a positive effect by reverting the evaluated 5XFAD EPM parameters to those shown by WT group (Figures 2d-f, Supplementary Table S4). I2-IR ligand treatment alone did not affect any of the EPM parameters studied, whereas co-treatment maintained the donepezil values. Treatments did not induce significant changes in EPM parameters evaluated in WT mice (Supplementary Table S4).

3.3 I2-IR ligand LSL60101 and donepezil ameliorate social deficits presented by 5XFAD mice.

To evaluate the effect of treatments on social behaviour, mice were subjected to the TCT. No differences in the number of entries to each chamber were determined in the habituation phase in any tested group (Figure 2g). On the contrary, mice spent more time in the intruder's chamber during the test phase in all experimental conditions (Figure 2h). When the social interaction was evaluated, 5XFAD mice spent significantly less time interacting with the intruder compared to the WT healthy control (Figure 2i). All treatments improved social impairments in 5XFAD treated groups by increasing the time of interaction compared to the

5XFAD controls, but only 5XFAD treated with donepezil reached significance (Figure 2i), whereas for LSL60101 $p < 0.06$ was calculated. WT treated mice presented no differences compared to WT controls.

3.4 I2-IR ligand LSL60101, but not donepezil, reduces A β plaques. By contrast, donepezil/LSL60101 attenuates A β pathology in 5XFAD mice.

The number of amyloid plaques in 5XFAD hippocampus and cortex and mice was assessed by histochemical staining with Thioflavin-S. LSL60101 induced significant decrease in the total number and area (%) covered by the plaques in 5XFAD mice compared to the 5XFAD controls, demonstrating a neuroprotective function of I2-IR ligand regarding the senile plaque formation. Treatment with donepezil did not reduce the number of amyloid plaques or area significantly in 5XFAD mice (Figures 3a, 3b-3c). The protein levels of A β determined by WB tended to decrease in all treated groups without reaching significance (Figure 3d, 3f). As expected, full-length APP protein levels were increased in 5XFAD mice compared to WT mice, and treatments did not modify protein expression (Figure 4a, 4h). Interestingly, alterations in the levels of proteins implicated in the APP processing showed complementary results in the combination of LSL60101 and donepezil treatment. In this line, the protein levels of C-terminal fragments (CTFs) were found significantly reduced in LSL60101 treated group compared to the 5XFAD controls, while LSL60101/donepezil treated group showed a significant decrease in CTFs compared with monotherapy (Figures 4b, 4h). The protein levels of phosphorylated amyloid precursor protein (p-APP) at Th668 were decreased significantly only for the combination of LSL60101/donepezil/ treated animals (Figures 4c, 4h). Soluble APP β (sAPP β) levels were found increased in 5XFAD controls compared to WT mice, confirming the amyloid pathology process. Furthermore, a significant decrease in LSL60101/donepezil treated group was determined (Figures 4d, 4h). Soluble APP α (sAPP α) levels were found increased after combination treatment when compared to 5XFAD controls or donepezil treated mice (Figures 4e, 4h). Regarding the levels of BACE1 (β -secretase) and ADAM10 (α -secretase), no significant differences were observed among the 5XFAD groups (Figures 4f, 4g, 4h). However, when the gene expression of enzymes implicated in amyloid degradation was studied, treatments slightly increased gene expression of *insulin-degrading*

enzyme (*IDE*), whereas *nepriylsin* (*Nep*) was only reduced in the donepezil and LSL60101 groups (Figure 4i).

3.5 I2-IR ligand LSL60101 and combination with donepezil reduce Tau hyperphosphorylation in 5XFAD mice.

Tau hyperphosphorylation, another major hallmark of AD, was evaluated in the hippocampus of the 5XFAD mice. I2-IR ligand LSL60101 and the co-treatment donepezil/LSL60101 decreased the Tau phosphorylation at the Ser404 and Ser396, diminutions that reached significance for the donepezil/LSL60101 treated 5XFAD mice. Of note, significant differences in p-Tau levels were also found between the donepezil/LSL60101 5XFAD treated mice and the donepezil or LSL60101 treated ones (Figures 3e, 3f).

3.6 Effects of LSL60101 on microglia activation and inflammatory markers expression.

In the AD brain, the formation of A β plaques leads to the activation of astrocytes and reactive gliosis. To examine changes in microglia reactivity, Iba-1 was determined by IHC experiments. Importantly, LSL60101 treatment resulted in a significant decrease in Iba-1 levels in the hippocampus (Figures 5a-5d) and in the cortex (Supplementary Figure S3) of 5XFAD mice, whereas donepezil did not affect Iba-1 immunoreactivity (Figures 5a-5d). LSL60101/donepezil combination reduced significantly Iba-1 levels in the cortex (Supplementary Figure S3), and in the DG area in the hippocampus (Figures 5a-5d). The gene expression of different inflammatory mediators was evaluated in the hippocampus of 5XFAD mice. In whole, 5XFAD mice presented an evident exacerbation of inflammatory response compared to WT mice, whereas treatments led to the upregulation of specific markers studied. No significant changes were determined in *Interleukin 1 β* (*Il-1 β*), *Interleukin 6* (*Il-6*) markers in treated groups compared to 5XFAD controls (Figure 5e). However, *Chemokine (C-C motif) ligand 12* (*Ccl12*) and *Interleukin 18* (*Il-18*) were found increased in LSL60101 group, and LSL60101/donepezil treated groups compared to 5XFAD controls (Figure 5e). Moreover, the gene expression of *Triggering receptor expressed on myeloid cells 2* (*Trem2*) was increased significantly after treatment with the I2-IR ligand LSL60101 and the combination-treated group (Figure 5f), confirming the results of *Il-18* and *Ccl12*.

3.6 LSL60101 effects on astroglial activation and synaptic dysfunction.

All treatments were able to attenuate astrogliosis in the hippocampus of 5XFAD brains by decreasing GFAP immunoreactivity in DG, CA1 and CA3 areas in 5XFAD mice groups in comparison with untreated mice (Figures 6a-d). Similar results were observed in cortex (Data not shown). Likewise, synaptic plasticity markers were evaluated by WB. Decreases in the protein levels of postsynaptic density protein 95 (PSD95) and synaptophysin (SYN) were determined in 5XFAD mice when compared to WT mice (Figures 6f-6h). I2-IR ligand LSL60101 increased PSD95 levels when compared to 5XFAD control (Figure 6f, 6h). SYN levels were found to increase in LSL60101 and donepezil/LSL60101 treated 5XFAD mice, reaching significance only for the combination-treated group. Donepezil treatment was not able to modify these markers significantly (Figure 6g, 6h).

4. DISCUSSION

The identification of new targets for AD treatment is required due to the lack of effective disease treatment. At present, AChEI are one of the standard therapeutic options clinically available for AD patients; however, those treatments provide only symptomatic benefit in AD (Sinforiani et al., 2003; Rosini et al., 2014). Fortunately, the number of disease-modifying drugs targeting AD hallmarks such as aducanumab (BIIB037), which is currently in phase 3 trials, is increasing (Cummings et al., 2020). Combination therapies of symptomatic and disease-modifying drugs have centred attention due to the multifactorial origin of the disease, and most current clinical trials combine donepezil with novel neuroprotective drugs (Frölich et al., 2019). However, it remains a challenge that must be addressed to unveil new strategies that could be more effective in disease-modifying treatment rather than address symptoms (Schmitt et al., 2004).

Several studies have described the symptomatic effects of donepezil in animal models of dementia and AD, but few *in vivo* studies have evaluated donepezil neuroprotective effects regarding the disease-modifying actions of this compound alone or in combination (Jiangbo and Liyun, 2018; Krishna et al., 2020; Yang et al., 2020; Ongnok et al., 2021). Here, we studied the effect of chronic low doses of an I2-IR ligand, donepezil, and their combination.

In the light of our studies, we demonstrated for the first time the neuroprotective effects of selective I2-IR ligands in the senescence-accelerated mouse prone 8 (SAMP8), a mouse model

of late-onset AD (Griñán-Ferré et al., 2019). LSL60101, a selective I2-IR ligand, has been shown to induce several biological effects associated with I2-IR occupancy and, most importantly, neuroprotective effects in the CNS (Menargues et al., 1994; Boronat et al., 1998; Casanovas et al., 2000; Sánchez-Blázquez et al., 2000). Therefore, it represents a suitable drug candidate to validate this receptor as a target for AD. Here, we demonstrated the efficacy of chronic low-dose I2-IR ligand LSL60101 treatment compared to donepezil by assessing the beneficial outcomes in a model of familial AD.

Cognitive abilities are the essential indicators to unveil pharmacological effects in AD. Firstly, chronic low-dose treatment with the I2-IR ligand LSL60101 or donepezil reversed the cognitive deficits presented by 7-month-old 5XFAD mice without affecting WT mice in the NORT paradigm. However, in the spatial memory test, only LSL60101 showed improvements in memory. Likewise, 5XFAD exhibited improved social behaviour after LSL60101 or donepezil treatment. In agreement with these results, donepezil has been shown to improve social interactions in scopolamine-induced memory impairments in mice (Riedel et al., 2009) and in drug-trials for AD (Boada-Rovira et al., 2004). Nevertheless, the beneficial effect of an I2-IR ligand treatment on social interaction deficits has not been described previously.

By contrast, I2-IR ligand LSL60101 did not modify anxiety-like behaviour, albeit previous studies have shown the *in vivo* anxiolytic and anti-depressant-like effects induced by I2-IR ligands (Finn et al., 2003; Tonello et al., 2012). Interestingly, the absence of anti-depressant effect after treatment with LSL60101 in healthy rats was recently described (Hernández-Hernández et al., 2020), further supporting our results since anxiety-like and depressive-like behaviour are strongly associated, sharing common molecular pathways (Gatt et al., 2009). In contrast, and according to literature (Fitzgerald et al., 2020), chronic treatment with donepezil showed beneficial effects on the anxiety-related disturbances exhibited by 5XFAD mice.

Recently, we reported that the amyloidogenic APP processing pathway was suppressed in SAMP8 and 5XFAD mice after treatment with novel I2-IR ligands, anticipating the role of I2-IR modulation in the A β biogenesis (Griñán-Ferré et al., 2019; Abás et al., 2020; Vasilopoulou et al., 2020b). Accordingly, in this study, we demonstrated for the first time that chronic low-dose treatment with I2-IR ligand LSL60101 attenuated the amyloid plaque burden in 5XFAD mice. In addition, A β plaques reduction was accompanied by a decrease in CTFs and A β hippocampal protein levels, as well as favourable modifications in APP processing after

treatment. Conversely, recently it was reported that the I2-IR ligand BU224 does not ameliorate A β amyloidosis in 5XFAD mice but improves memory (Mirzaei et al., 2020). In contrast with LSL60101 like molecules, BU224 blocked the memory-enhancing effect of agmatine in memory deficits induced by A β ₁₋₄₂ in mice (Kotagale et al., 2020). These discrepancies between I2-IR ligands can be explained by differences in compound administration conditions such as dose, time (sub-chronic vs. chronic), and administration route. Thus, we hypothesise that low doses of LSL60101, as well as the chronicity of treatment, have a clear beneficial effect on amyloid burden because of differential characteristics among I2-IR ligands (Sánchez-Blázquez et al., 2000; Garau et al., 2013).

Several studies have demonstrated the effect of donepezil on A β pathology in AD models, reporting either beneficial changes (Dong et al., 2009; Takada-Takatori et al., 2019) or lack of effect (Ju and Tam, 2020). Here, low-dose donepezil treatment did not induce significant changes on A β plaques nor APP processing in 7-month-old 5XFAD. Of note, co-administration of I2-IR ligand LSL60101 and donepezil showed a greater effect on APP processing than monotherapy. Regarding the A β degradation, the co-treatment LSL60101/donepezil induced an increase in A β degradation enzymes gene expression in 5XFAD mice, which was not determined in the other treated groups. To sum up, this is the first time an I2-IR ligand was shown to effectively reduce the A β plaques in the *in vivo* mice model of AD.

The presence of p-Tau, another major AD hallmark, in the 5XFAD model is supported by previous studies suggesting that tau pathology may be downstream from A β pathology (Blanchard et al., 2003; Saul et al., 2013). I2-IR ligand LSL60101 ameliorated tau pathology in the hippocampus of 5XFAD mice. Interestingly, it was shown recently that chronic treatment with idazoxan, a mixed α 2/I2 ligand, reduced p-Tau reversing cognitive deficits in AD mice because of its α 2 blockade action (Zhang et al., 2020). In this case, the effect of LSL60101 on Tau pathology can be attributed to its I2 selectivity, more than to the α 2 one. Surprisingly, the p-Tau reduction reached significance in the 5XFAD mice treated with the combination of LSL60101 with donepezil demonstrating, in this case, a putative additive effect of the drugs on tau pathology. Indeed, amelioration of tau pathology has been induced in AD animal models both by donepezil (Yoshiyama et al., 2010) and by I2-IR ligand treatments (Griñán-Ferré et al., 2019; Vasilopoulou et al., 2020b). It is possible that the activation of distinct

molecular pathways by the two molecules with different modes of actions resulted in a remarkable p-Tau reduction observed in the donepezil/LSL60101 treated mice group.

It is well-established that A β accumulation jointly with p-Tau increases microglial activation and inflammatory mediators' production in AD brains (Akiyama et al., 2000; Serrano-Pozo et al., 2011; Zhang and Jiang, 2015). On the one hand, chronic low-dose LSL60101 treatment reduced microgliosis in 5XFAD mice in contrast to the standard of care donepezil, explaining the decrease in the amyloid deposition that in turn would lead to a decrease in gliotic response after LSL60101 treatment. On the other hand, inflammatory gene expression increase (*Il-18* and *Ccl12*) was observed after treatment with I2-IR ligand LSL60101 and LSL60101/donepezil, but not with donepezil. Interestingly, this was further supported by a significant upregulation of *Trem2* gene expression determined in the LSL60101 treated mice, further confirming the neuroinflammatory modulation by I2-IR ligand LSL60101 (Hwang et al., 2010; Griñán-Ferré et al., 2019; Vasilopoulou et al., 2020a). In fact, increased *Trem2* expression has been shown to reprogram microglia responsivity mediating microglial cytokine release, migration, and clearance of A β deposits, ameliorating neuropathological and behavioural deficits of AD mouse models (Lee et al., 2018; Zhao et al., 2018).

It has been described that the I2-IR modulate the expression of astrocyte marker GFAP, especially considering their primary location in astrocytes (Regunathan et al., 1993; Olmos et al., 1994; Regunathan et al., 1999). GFAP diminution was observed in vivo and in vitro after treatment with selective I2-IR ligands (Siemian et al., 2018; Griñán-Ferré et al., 2019; Vasilopoulou et al., 2020b;). In agreement with those results, chronic low-dose treatment with I2-IR ligand LSL60101 attenuated astrogliosis in 5XFAD mice. By contrast, it has been shown that chronic treatment with LSL60101 increased GFAP immunoreactivity (Alemany et al., 1995), resulting in reactive astrogliosis and preventing motoneuron cell death in neonatal rats (Casanovas et al., 2000). However, here, in a neurodegenerative landscape provided by the 5XFAD model, the diminution of GFAP reactivity ran in parallel with the attenuation of the A β pathology and microglial activation observed after LSL60101 and donepezil treatment, given further support to the beneficial effects of I2-IR ligand on mice behaviour. Ultimately, we demonstrated that chronic low-dose treatment with I2-IR ligand and donepezil enhanced synaptic plasticity, further supporting the cognitive and behavioural improvement induced by the LSL60101 in 5XFAD mice.

Nevertheless, one limitation of our study was that only female 5XFAD mice were used to establish the protective effect of LSL60101 on AD-hallmarks and cognition. It would be of great interest to carry out experiments on male mice, once we have demonstrated the disease-modifying effects promoted by LSL60101 in a female mice model of AD.

5. CONCLUSIONS

Collectively, we report that chronic low-dose treatment with I2-IR ligand LSL60101 reversed cognitive deficits in 5XFAD mice, altering AD neuropathological hallmarks, including glial activation and synaptic dysfunction. Strikingly, treatment with I2-IR ligand LSL60101 was found to exert greater beneficial effects under the neurodegenerative process caused by A β pathology than donepezil. However, combination treatment only showed discrete synergistic effects at the molecular level (e.g., tau hyperphosphorylation or synaptic plasticity), suggesting that increased dosage and/or duration of the treatment may be able to produce better effects on both behaviour and AD-hallmarks, targeting simultaneously pathological and symptomatic reliefs. In conclusion, our findings demonstrate the therapeutic potential of the I2-IR for AD treatment as a disease-modifying single therapy and provide new insights into their efficacy.

REFERENCES

- Abás, S., Erdozain, A.M., Keller, B., Rodríguez-Arévalo, S., Callado, L.F., García-Sevilla, J.A., et al. (2017). Neuroprotective Effects of a Structurally New Family of High Affinity Imidazoline I₂ Receptor Ligands. *ACS Chem. Neurosci.* 8: 737–742.
- Abás, S., Rodríguez-Arévalo, S., Bagán, A., Griñán-Ferré, C., Vasilopoulou, F., Brocos-Mosquera, I., et al. (2020). Bicyclic α -Iminophosphonates as High Affinity Imidazoline I₂ Receptor Ligands for Alzheimer's Disease. *J. Med. Chem.* 63: 3610–3633.
- Akiyama, H., Barger, S., Barnum, S., Bradt, B., Bauer, J., Cole, G.M., et al. (2000). Inflammation and Alzheimer's disease. *Neurobiol. Aging* 21: 383–421.
- Aleman, R., Olmos, G., Escribá, P. V., Menargues, A., Obach, R., and García-Sevilla, J.A. (1995). LSL 60101, a selective ligand for imidazoline I₂ receptors, on glial fibrillary acidic protein concentration. *Eur. J. Pharmacol.* 280: 205–210.

- Archer, J. (1973). Tests for emotionality in rats and mice: A review. *Anim. Behav.* *21*: 205–235.
- Blanchard, V., Moussaoui, S., Czech, C., Touchet, N., Bonici, B., Planche, M., et al. (2003). Time sequence of maturation of dystrophic neurites associated with Abeta deposits in APP/PS1 transgenic mice. *Exp. Neurol.* *184*: 247–263.
- Boada-Rovira, M., Brodaty, H., Cras, P., Baloyannis, S., Emre, M., Zhang, R., et al. (2004). Efficacy and Safety of Donepezil in Patients with Alzheimer's Disease. *Drugs Aging* *21*: 43–53.
- Boronat, M.A., Olmos, G., and García-Sevilla, J.A. (1998). Attenuation of tolerance to opioid-induced antinociception and protection against morphine-induced decrease of neurofilament proteins by idazoxan and other I2-imidazoline ligands. *Br. J. Pharmacol.* *125*: 175–185.
- Bousquet, P., Hudson, A., García-Sevilla, J.A., and Li, J.X. (2020). Imidazoline receptor system: The past, the present, and the future. *Pharmacol. Rev.* *72*: 50–79.
- Bradford, M.M. (1976). A rapid and sensitive method for the quantitation of microgram quantities of protein utilizing the principle of protein-dye binding. *Anal. Biochem.* *72*: 248–254.
- Casanovas, A., Olmos, G., Ribera, J., Boronat, M.A., Esquerda, J.E., and García-Sevilla, J.A. (2000). Induction of reactive astrogliosis and prevention of motoneuron cell death by the I(2)-imidazoline receptor ligand LSL 60101. *Br. J. Pharmacol.* *130*: 1767–1776.
- Companys-Aleman, J., Turcu, A.L., Bellver-Sanchis, A., Loza, M.I., Brea, J.M., Canudas, A.M., et al. (2020). A novel NMDA receptor antagonist protects against cognitive decline presented by senescent mice. *Pharmaceutics* *12*: 1–17.
- Cummings, J., Lee, G., Ritter, A., Sabbagh, M., and Zhong, K. (2020). Alzheimer's disease drug development pipeline: 2020. *Alzheimer's Dement. Transl. Res. Clin. Interv.* *6*: 1–29.
- Curtis, M.J., Alexander, S., Cirino, G., Docherty, J.R., George, C.H., Giembycz, M.A., et al. (2018). Experimental design and analysis and their reporting II: updated and simplified guidance for authors and peer reviewers. *Br. J. Pharmacol.* *175*: 987–993.
- DeTure, M.A., and Dickson, D.W. (2019). The neuropathological diagnosis of Alzheimer's disease. *Mol. Neurodegener.* *14*: 32.
- Dickson, D.W., and Rogers, J. (1992). Neuroimmunology of Alzheimer's disease: A conference report. *Neurobiol. Aging* *13*: 793–798.
- Dong, H., Yuede, C.M., Coughlan, C.A., Murphy, K.M., and Csernansky, J.G. (2009). Effects of donepezil on amyloid-beta and synapse density in the Tg2576 mouse model of Alzheimer's disease. *Brain Res.* *1303*: 169–178.

- Ennaceur, A., and Delacour, J. (1988). A new one-trial test for neurobiological studies of memory in rats. 1: Behavioral data. *Behav. Brain Res.* *31*: 47–59.
- Finn, D.P., Martí, O., Harbuz, M.S., Vallès, A., Belda, X., Márquez, C., et al. (2003). Behavioral, neuroendocrine and neurochemical effects of the imidazoline I2 receptor selective ligand BU224 in naive rats and rats exposed to the stress of the forced swim test. *Psychopharmacology (Berl)*. *167*: 195–202.
- Fitzgerald, P.J., Hale, P.J., Ghimire, A., and Watson, B.O. (2020). The cholinesterase inhibitor donepezil has antidepressant-like properties in the mouse forced swim test. *Transl. Psychiatry* *10*: 255.
- Frölich, L., Atri, A., Ballard, C., Tariot, P.N., Molinuevo, J.L., Boneva, N., et al. (2019). Open-Label, Multicenter, Phase III Extension Study of Idalopirdine as Adjunctive to Donepezil for the Treatment of Mild-Moderate Alzheimer's Disease. *J. Alzheimers. Dis.* *67*: 303–313.
- Garau, C., Miralles, A., Garcia-Sevilla, J. a, and García-Sevilla, J. a (2013). Chronic treatment with selective I2-imidazoline receptor ligands decreases the content of pro-apoptotic markers in rat brain. *J. Psychopharmacol.* *27*: 123–34.
- Garcia-Sevilla, J., Escriba, P., Walzer, C., Bouras, C., and Guimon, J. (1998). Imidazoline receptor proteins in brains of patients with Alzheimer's disease. *Neurosci. Lett.* *247*: 95–98.
- Gatt, J.M., Nemeroff, C.B., Dobson-Stone, C., Paul, R.H., Bryant, R.A., Schofield, P.R., et al. (2009). Interactions between BDNF Val66Met polymorphism and early life stress predict brain and arousal pathways to syndromal depression and anxiety. *Mol. Psychiatry* *14*: 681–695.
- Giacobini, E. (2000). Cholinesterase Inhibitors Stabilize Alzheimer Disease. *Neurochem. Res.* *25*: 1185–1190.
- Griñán-Ferré, C., Izquierdo, V., Otero, E., Puigoriol-Illamola, D., Corpas, R., Sanfeliu, C., et al. (2018). Environmental Enrichment Improves Cognitive Deficits, AD Hallmarks and Epigenetic Alterations Presented in 5xFAD Mouse Model. *Front. Cell. Neurosci.* *12*: 224.
- Griñán-Ferré, C., Palomera-Ávalos, V., Puigoriol-Illamola, D., Camins, A., Porquet, D., Plá, V., et al. (2016). Behaviour and cognitive changes correlated with hippocampal neuroinflammation and neuronal markers in female SAMP8, a model of accelerated senescence. *Exp. Gerontol.* *80*: 57–69.
- Griñán-Ferré, C., Vasilopoulou, F., Abás, S., Rodríguez-Arévalo, S., Bagán, A., Sureda, F.X., et al. (2019). Behavioral and Cognitive Improvement Induced by Novel Imidazoline I2 Receptor Ligands in Female SAMP8 Mice. *Neurotherapeutics* *16*: 416–431.

- Grossberg, G.T. (2003). Cholinesterase inhibitors for the treatment of Alzheimer's disease: getting on and staying on. *Curr. Ther. Res. Clin. Exp.* *64*: 216–235.
- Hernández-Hernández, E., García-Sevilla, J.A., and García-Fuster, M.J. (2020). Exploring the antidepressant-like potential of the selective I2-imidazoline receptor ligand LSL 60101 in adult male rats. *Pharmacol. Reports*.
- Hwang, J., Hwang, H., Lee, H.-W., and Suk, K. (2010). Microglia signaling as a target of donepezil. *Neuropharmacology* *58*: 1122–1129.
- Jawhar, S., Trawicka, A., Jenneckens, C., Bayer, T.A., and Wirths, O. (2012). Motor deficits, neuron loss, and reduced anxiety coinciding with axonal degeneration and intraneuronal A β aggregation in the 5XFAD mouse model of Alzheimer's disease. *Neurobiol. Aging* *33*: 196.e29–40.
- Jiangbo, N., and Liyun, Z. (2018). Effect of donepezil hydrochloride & aerobic exercise training on learning and memory and its mechanism of action in an Alzheimer's disease rat model. *Pak. J. Pharm. Sci.* *31*: 2897–2901.
- Ju, Y., and Tam, K.Y. (2020). 9R, the cholinesterase and amyloid beta aggregation dual inhibitor, as a multifunctional agent to improve cognitive deficit and neuropathology in the triple-transgenic Alzheimer's disease mouse model. *Neuropharmacology* *181*: 108354.
- Kim, H.G., Moon, M., Choi, J.G., Park, G., Kim, A.-J., Hur, J., et al. (2014). Donepezil inhibits the amyloid-beta oligomer-induced microglial activation in vitro and in vivo. *Neurotoxicology* *40*: 23–32.
- Kotagale, N., Dixit, M., Garmelwar, H., Bhondekar, S., Umekar, M., and Taksande, B. (2020). Agmatine reverses memory deficits induced by A β 1–42 peptide in mice: A key role of imidazoline receptors. *Pharmacol. Biochem. Behav.* *196*:
- Krishna, K.V., Saha, R.N., and Dubey, S.K. (2020). Biophysical, Biochemical, and Behavioral Implications of ApoE3 Conjugated Donepezil Nanomedicine in a A β 1–42 Induced Alzheimer's Disease Rat Model. *ACS Chem. Neurosci.*
- Landel, V., Baranger, K., Virard, I., Loriod, B., Khrestchatsky, M., Rivera, S., et al. (2014). Temporal gene profiling of the 5XFAD transgenic mouse model highlights the importance of microglial activation in Alzheimer's disease. *Mol. Neurodegener.* *9*: 33.
- Lee, C.Y.D., Daggett, A., Gu, X., Jiang, L.L., Langfelder, P., Li, X., et al. (2018). Elevated TREM2 Gene Dosage Reprograms Microglia Responsivity and Ameliorates Pathological Phenotypes in Alzheimer's Disease Models. *Neuron* *97*: 1032-1048.e5.

- Lilley, E., Stanford, S.C., Kendall, D.E., Alexander, S.P.H., Cirino, G., Docherty, J.R., et al. (2020). ARRIVE 2.0 and the British Journal of Pharmacology: Updated guidance for 2020. *Br. J. Pharmacol.* *177*: 3611–3616.
- Mehta, M., Adem, A., and Sabbagh, M. (2012). New acetylcholinesterase inhibitors for Alzheimer's disease. *Int. J. Alzheimers. Dis.* *2012*: 728983.
- MERAZ RIOS, M.A., TORAL-RIOS, D., FRANCO-BOCANEGRA, D., VILLEDA-HERNÁNDEZ, J., and CAMPOS-PEÑA, V. (2013). Inflammatory process in Alzheimer's Disease . *Front. Integr. Neurosci.* *7*: 59.
- Mirzaei, N., Mota, B.C., Birch, A.M., Davis, N., Romero-Molina, C., Katsouri, L., et al. (2020). Imidazoline ligand BU224 reverses cognitive deficits, reduces microgliosis and enhances synaptic connectivity in a mouse model of Alzheimer's disease. *Br. J. Pharmacol.*
- Murray, M.E., Graff-Radford, N.R., Ross, O.A., Petersen, R.C., Duara, R., and Dickson, D.W. (2011). Neuropathologically defined subtypes of Alzheimer's disease with distinct clinical characteristics: a retrospective study. *Lancet. Neurol.* *10*: 785–796.
- Oakley, H., Cole, S.L., Logan, S., Maus, E., Shao, P., Craft, J., et al. (2006). Intraneuronal β -amyloid aggregates, neurodegeneration, and neuron loss in transgenic mice with five familial Alzheimer's disease mutations: Potential factors in amyloid plaque formation. *J. Neurosci.* *26*: 10129–10140.
- Olmos, G., Alemany, R., Escriba, P.V., and García-Sevilla, J.A. (1994). The effects of chronic imidazoline drug treatment on glial fibrillary acidic protein concentrations in rat brain. *Br. J. Pharmacol.* *111*: 997–1002.
- Ongnok, B., Khuanjing, T., Chunchai, T., Kerdphoo, S., Jaiwongkam, T., Chattipakorn, N., et al. (2021). Donepezil provides neuroprotective effects against brain injury and Alzheimer's pathology under conditions of cardiac ischemia/reperfusion injury. *Biochim. Biophys. Acta. Mol. Basis Dis.* *1867*: 165975.
- Puzzo, D., Gulisano, W., Palmeri, A., and Arancio, O. (2015). Rodent models for Alzheimer's disease drug discovery. *Expert Opin. Drug Discov.* *10*: 703–711.
- Regunathan, S., Feinstein, D.L., and Reis, D.J. (1993). Expression of non-adrenergic imidazoline sites in rat cerebral cortical astrocytes. *J. Neurosci. Res.* *34*: 681–688.
- Regunathan, S., Feinstein, D.L. and Reis, D.J. (1999). Anti-Proliferative and Anti-Inflammatory Actions of Imidazoline Agents: Imidazoline Receptors Involved?. *Annals of the New York Academy of Sciences*, *881*: 410-419.

- Riedel, G., Kang, S.H., Choi, D.Y., and Platt, B. (2009). Scopolamine-induced deficits in social memory in mice: Reversal by donepezil. *Behav. Brain Res.* *204*: 217–225.
- Rosini, M., Simoni, E., Minarini, A., and Melchiorre, C. (2014). Multi-target design strategies in the context of Alzheimer's disease: acetylcholinesterase inhibition and NMDA receptor antagonism as the driving forces. *Neurochem. Res.* *39*: 1914–1923.
- Ruiz, J., Martín, I., Callado, L.F., Meana, J.J., Barturen, F., and García-Sevilla, J.A. (1993). Non-adrenoceptor [3H]imidazoxan binding sites (I₂-imidazoline sites) are increased in postmortem brain from patients with Alzheimer's disease. *Neurosci. Lett.* *160*: 109–112.
- Sánchez-Blázquez, P., Boronat, M.A., Olmos, G., García-Sevilla, J.A., and Garzón, J. (2000). Activation of I(2)-imidazoline receptors enhances supraspinal morphine analgesia in mice: a model to detect agonist and antagonist activities at these receptors. *Br. J. Pharmacol.* *130*: 146–152.
- Saul, A., Sprenger, F., Bayer, T.A., and Wirths, O. (2013). Accelerated tau pathology with synaptic and neuronal loss in a novel triple transgenic mouse model of Alzheimer's disease. *Neurobiol. Aging* *34*: 2564–2573.
- Schmitt, B., Bernhardt, T., Moeller, H.-J., Heuser, I., and Frölich, L. (2004). Combination therapy in Alzheimer's disease: a review of current evidence. *CNS Drugs* *18*: 827–844.
- Selkoe, D.J. (2008). Soluble oligomers of the amyloid beta-protein impair synaptic plasticity and behavior. *Behav. Brain Res.* *192*: 106–113.
- Serrano-Pozo, A., Frosch, M.P., Masliah, E., and Hyman, B.T. (2011). Neuropathological alterations in Alzheimer disease. *Cold Spring Harb. Perspect. Med.* *1*: a006189.
- Siemian, J.N., LaMacchia, Z.M., Spreuer, V., Tian, J., Ignatowski, T.A., Paez, P.M., Zhang, Y., Li, J.X. (2018). The imidazoline I₂ receptor agonist 2-BFI attenuates hypersensitivity and spinal neuroinflammation in a rat model of neuropathic pain. *Biochem Pharmacol.* *153*:260-268.
- Sinforiani, E., Banchieri, L.M., Zucchella, C., Bernasconi, L., and Nappi, G. (2003). Cholinesterase inhibitors in Alzheimer's disease: efficacy in a non-selected population. *Funct. Neurol.* *18*: 233–237.
- Takada-Takatori, Y., Nakagawa, S., Kimata, R., Nao, Y., Mizukawa, Y., Urushidani, T., et al. (2019). Donepezil modulates amyloid precursor protein endocytosis and reduction by up-regulation of SNX33 expression in primary cortical neurons. *Sci. Rep.* *9*: 11922.

- Tonello, R., Villarinho, J.G., Silva Sant'Anna, G. da, Tamiozzo, L., Machado, P., Trevisan, G., et al. (2012). The potential antidepressant-like effect of imidazoline I₂ ligand 2-BFI in mice. *Prog. Neuro-Psychopharmacology Biol. Psychiatry* 37: 15–21.
- Vasilopoulou, F., Bagan, A., Rodriguez-Arevalo, S., Escolano, C., Griñán-Ferré, C., and Pallàs, M. (2020a). Amelioration of BPSD-like phenotype and cognitive decline in SAMP8 mice model accompanied by molecular changes after treatment with I₂-imidazoline receptor ligand MCR5. *Pharmaceutics* 12:.
- Vasilopoulou, F., Griñán-Ferré, C., Rodríguez-Arévalo, S., Bagán, A., Abás, S., Escolano, C., et al. (2020b). I₂ imidazoline receptor modulation protects aged SAMP8 mice against cognitive decline by suppressing the calcineurin pathway. *GeroScience* 27–31.
- Walf, A.A., and Frye, C.A. (2007). The use of the elevated plus maze as an assay of anxiety-related behavior in rodents. *Nat. Protoc.* 2: 322–328.
- Walsh, D.M., and Selkoe, D.J. (2004). Oligomers on the brain: the emerging role of soluble protein aggregates in neurodegeneration. *Protein Pept. Lett.* 11: 213–228.
- Yang, H., Mu, W., Wei, D., Zhang, Y., Duan, Y., Gao, J. xiao, et al. (2020). A Novel Targeted and High-Efficiency Nanosystem for Combinational Therapy for Alzheimer's Disease. *Adv. Sci.* 7: 1–13.
- Yoshiyama, Y., Kojima, A., Ishikawa, C., and Arai, K. (2010). Anti-inflammatory action of donepezil ameliorates tau pathology, synaptic loss, and neurodegeneration in a tauopathy mouse model. *J. Alzheimers. Dis.* 22: 295–306.
- Zhang, F., Gannon, M., Chen, Y., Yan, S., Zhang, S., Feng, W., et al. (2020). β -amyloid redirects norepinephrine signaling to activate the pathogenic GSK3 β /tau cascade. *Sci. Transl. Med.* 12: eaay6931.
- Zhang, F., and Jiang, L. (2015). Neuroinflammation in Alzheimer's disease. *Neuropsychiatr. Dis. Treat.* 11: 243–256.
- Zhao, Y., Wu, X., Li, X., Jiang, L.-L., Gui, X., Liu, Y., et al. (2018). TREM2 Is a Receptor for β -Amyloid that Mediates Microglial Function. *Neuron* 97: 1023-1031.e7.

Figure legends

Figure 1. Effects of low-dose chronic treatment with I2-IR LSL60101, Donepezil and co-administration on cognitive status in 5XFAD and WT mice. (a) Scheme of experimental design. **Results of NORT:** Discrimination index calculated by using exploration time for novel and familiar object **(b)** in the short-term term memory test session (2h) (WT, n=10-12 per group; 5XFAD n=11-12 per group; Two-way ANOVA with Tukey post hoc analysis; genotype effect, $F(1,81)=4.52$, $P=0.0366$; treatment effect, $F(3,81)=8.27$, $P<0.0001$; interaction, $F(3,81)=6.0$, $P=0.0009$) **(c)** in the long-term memory test session (24h) (WT, n=10-12 per group; 5XFAD n=10-12 per group; Two-way ANOVA with Tukey post hoc analysis; genotype effect, $F(1,79)=16.86$, $P<0.0001$; treatment effect, $F(3,79)=1.82$, $P=0.1504$; interaction, $F(3,79)=6.06$, $P=0.0009$). **Results of MWM: (d)** Distance to target (platform) (cm) during the training session (WT n=10-11 per group; 5XFAD n=10-12 per group; Two-way ANOVA with Tukey post hoc analysis for each day; Day 5: genotype effect, $F(1,80)=2.34$, $P=0.12$; treatment effect, $F(3,80)=3.88$, $P=0.01$; interaction, $F(3,80)=2.20$, $p=0.09$) **(e)** Quadrant preference in the test session as time (%) spent in each quadrant WT n=9-12 per group; 5XFAD n=10-12 per group; One-way ANOVA with Tukey post hoc analysis between Quadrants for each experimental group) **(f)** Time (%) spent in platform quadrant in the test session (WT n=9-12 per group; 5XFAD n=10-12 per group; Two-way ANOVA with Tukey post hoc analysis; genotype effect, $F(1,77)=3.9$, $P=0.05$; treatment effect, $F(3,77)=1.66$, $P=0.18$; interaction, $F(3,77)=7.89$, $p=0.0001$) **(g)** Latency to target (platform) (sec) in the test session (WT n=9-12 per group; 5XFAD n=10-12 per group; Two-way ANOVA with Tukey post hoc analysis) **(h)** Representative images of trajectory during memory test. Bars represent mean \pm SEM; * $P<0.05$.

Figure 2. Effects of low-dose chronic treatments I2-IR LSL60101, Donepezil and co-administration on behavioral and social status in 5XFAD mice and WT controls. Results of OF: (a) Locomotor activity measured as distance travelled (cm) (WT n=10-12 per group; 5XFAD n=11-12 per group; Two-way ANOVA with Tukey post hoc analysis) **(b)** Time spent in the center (sec) (WT n=10-12 per group; 5XFAD n=9-11 per group; Two-way ANOVA with post hoc analysis; genotype effect, $F(1,79)=5.972$, $P=0.0168$; treatment effect, $F(3,79)=4.79$, $P=0.0040$; interaction, $F(3,79)=4.14$, $P=0.0088$) **(c)** number of rearings (WT n=11-12 per group;

5XFAD n=10-12 per group; Two-way ANOVA with Tukey post hoc analysis; genotype effect, $F(1,83)=11.99$, $P=0.0008$; treatment effect, $F(3,83)=2.93$, $P=0.00382$; interaction, $F(3,83)=4.59$, $p=0.0051$). **Results of EPM: (d)** Time (%) spent in Open Arms (WT n=11-12 per group; 5XFAD n=10-12 per group; Two-way ANOVA with Tukey post hoc analysis; genotype effect, $F(1,81)=87.45$, $P<0.0001$; treatment effect, $F(3,81)=4.24$, $P=0.0078$; interaction, $F(3,81)=5.78$, $p=0.0012$) **(e)** Time (%) spent in closed arms (WT n=11-12 per group; 5XFAD n=10-12 per group; Two-way ANOVA with post hoc analysis: genotype effect, $F(1,83)=70.56$, $P<0.0001$; treatment effect, $F(3,83)=3.31$, $P=0.024$; interaction, $F(3,83)=5.93$, $P=0.0010$) **(f)** number of rearings (WT n=11-12 per group; 5XFAD n=11-12 per group; Two-way ANOVA with post hoc analysis; genotype effect, $F(1,83)=22.41$, $P<0.0001$; treatment effect, $F(3,83)=6.30$, $P=0.0007$; interaction, $F(3,83)=2.36$, $P=0.0775$). **Results of TCT: (g)** Entries in chambers (A1, A2) in the habituation phase (n) (WT n=11-12 per group; 5XFAD n=11-12 per group; Unpaired Student's t-test) **(h)** Time in chambers (Empty, Stranger) during the test session (WT n=10-11 per group; 5XFAD n=9-11 per group; Unpaired Student's t-test) **(i)** time of interaction with intruder (sec) in the test session (WT n=11-12 per group; 5XFAD n=10-11 per group Two-way ANOVA; genotype effect, $F(1,78)=0.160$, $P=0.6911$; treatment effect, $F(3,78)=0.65$, $P=0.58$; interaction, $F(3,78)=$, $p=0.0018$). Bars represent mean \pm SEM; * $P<0.05$;

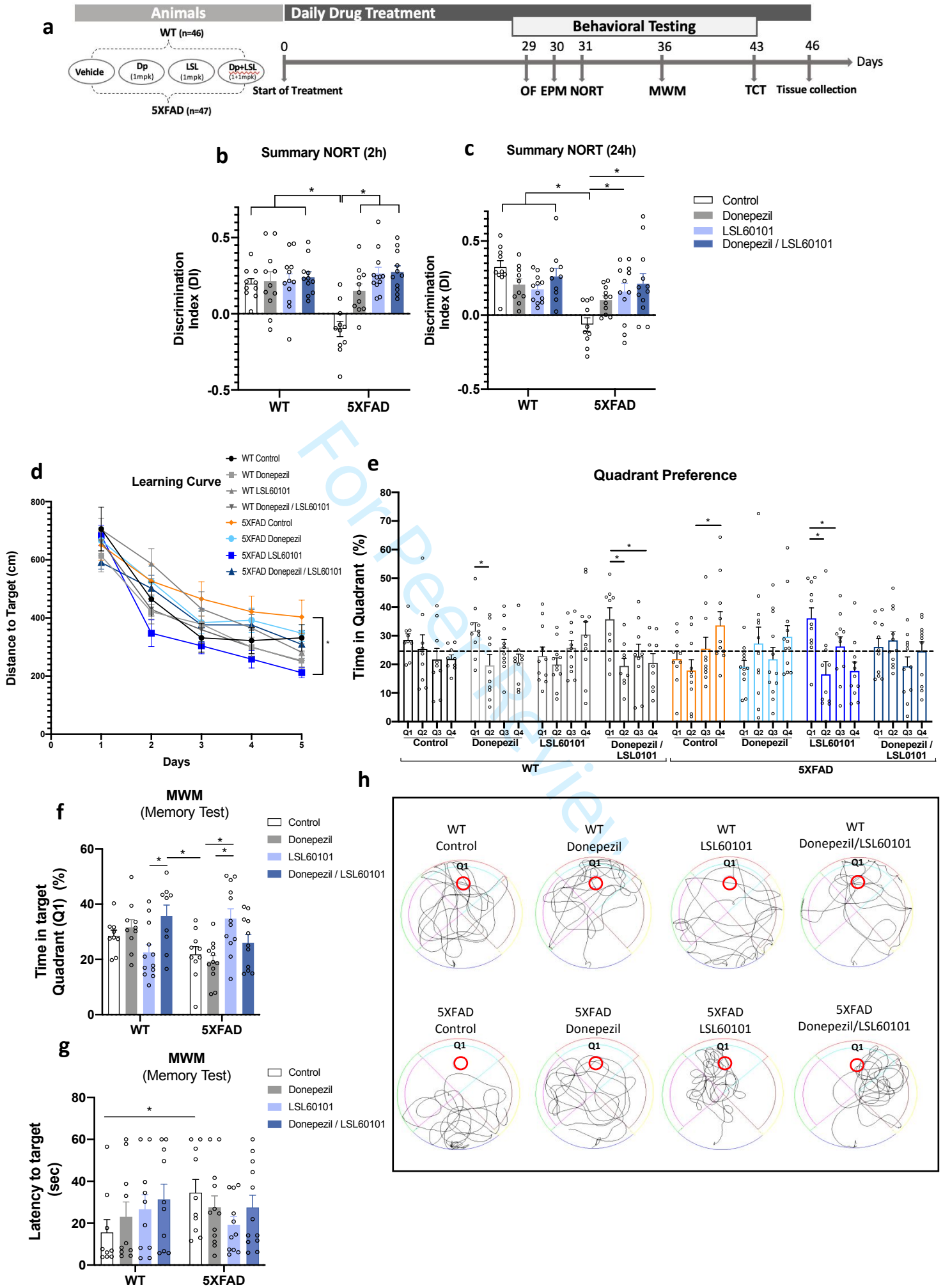
Figure 3. Effects of low dose chronic treatments I2-IR LSL60101, donepezil and co-administration on AD hallmarks in 5XFAD mice. (a) Representative images of thioflavin-S staining of amyloid plaques and quantification of **(b)** amyloid plaques number in cortex and hippocampus **(c)** and area (%) covered by plaques in the DG area of the hippocampus in the 5XFAD mice. Data are presented as the mean \pm SEM, and each dot represents one mouse (n=5 per group); averaged from 2-3 sections from the same brain area/animal. Representative Western blot and quantifications **(d-f)** for β -Amyloid, p-Tau(Ser404) and p-Tau(ser396) in the hippocampus of 5XFAD mice. Values in bar graphs are adjusted to 100% for protein levels of the control WT or the control 5XFAD. Bars represent mean \pm SEM. Student's t-test or one-way ANOVA with Tukey post hoc analysis, * $P<0.05$; n=5-6 per group. DG: Dentate gyrus.

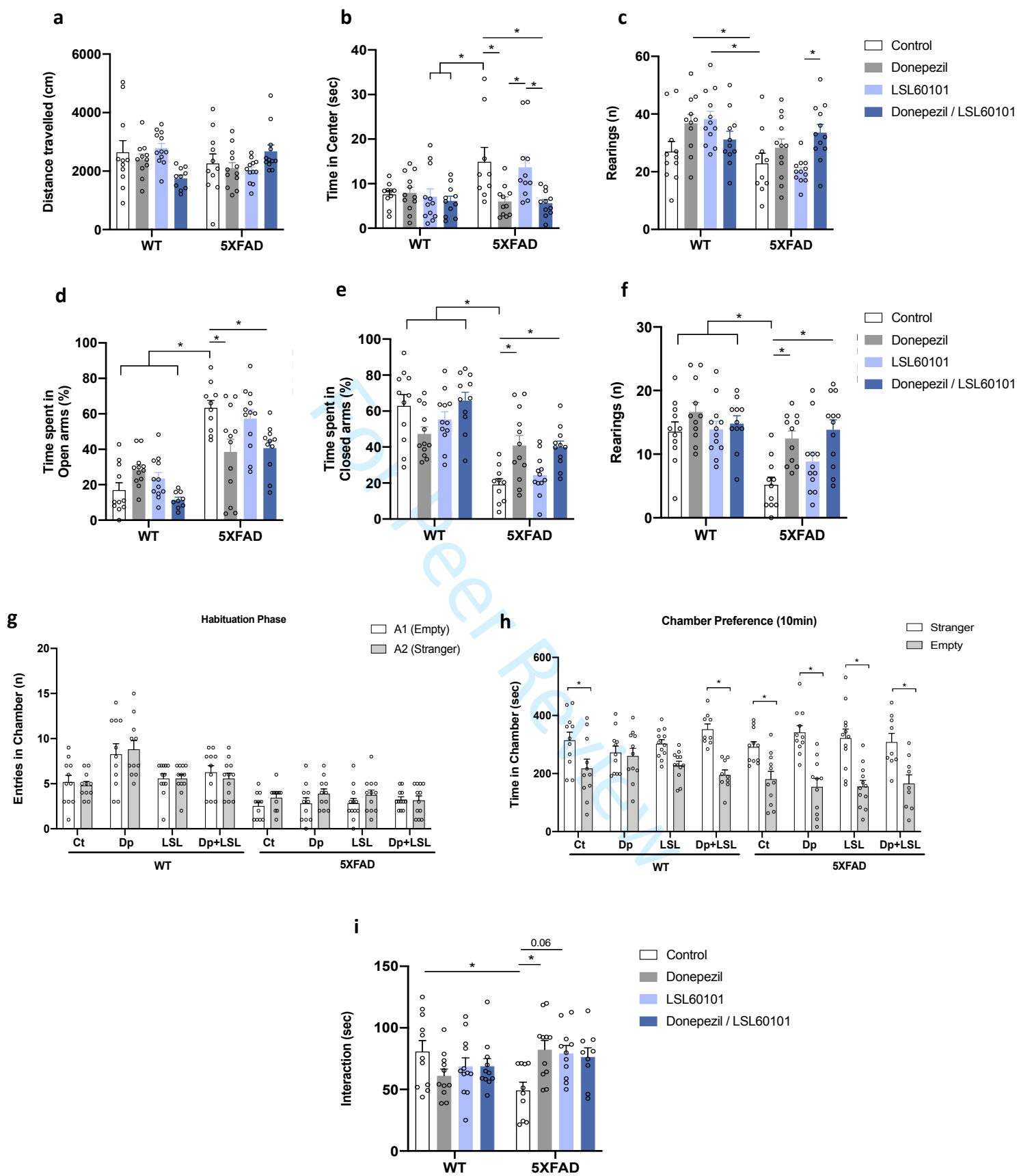
Figure 4. Effects of low dose chronic treatments I2-IR LSL60101, donepezil and co-administration on A β pathology and APP processing in 5XFAD mice. Representative Western Blots and Quantifications for (a-h) FL-APP, CTFs, p-APP, sAPP β , sAPP α , BACE 1, ADAM10 in

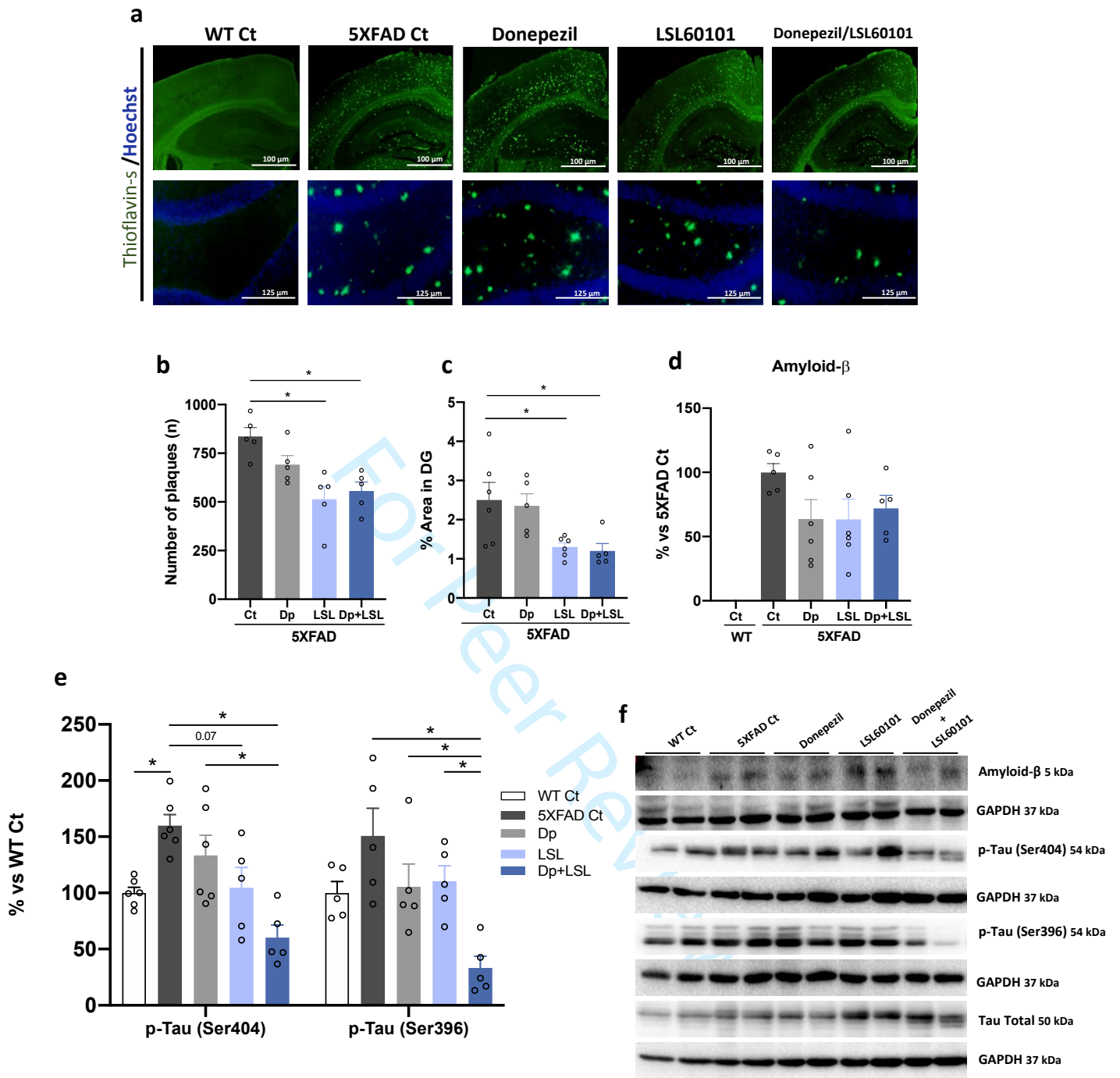
the hippocampus of 5XFAD mice. Values in bar graphs are adjusted to 100% for protein levels of the control WT or the control 5XFAD. Representative gene expression in the hippocampus of the 5XFAD mice for **(i)** *IDE*, *Nep*. Gene expression levels were determined by real-time PCR. Values in bar graphs are adjusted to 100% for relative gene expression of the WT control. Bars represent mean \pm SEM. Unpaired Student's t-test or one-way ANOVA with Tukey post hoc analysis, * $P < 0.05$; $n = 5-6$ per group.

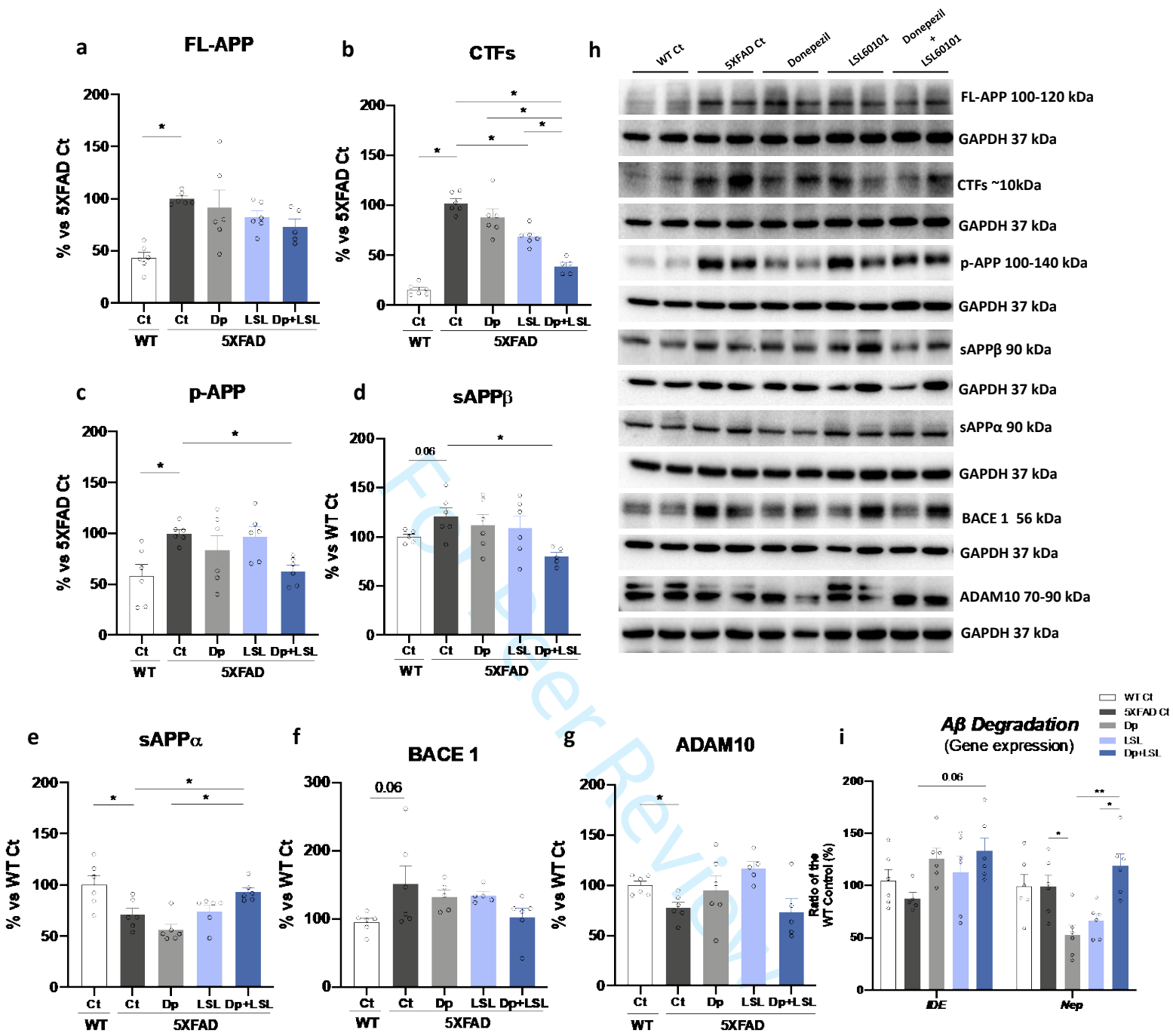
Figure 5. Effects of low dose chronic treatments I2-IR LSL60101, donepezil and co-administration on microgliosis and inflammatory markers in 5XFAD mice. **(a)** Representative images of Iba-1 immunostaining and quantification **(b-d)** in DG, CA1, CA3 areas of the hippocampus of the 5XFAD mice. Data are presented as the mean \pm SEM of relative fluorescent intensity of the positive cells averaged from 2-3 different sections from the same brain area/animal and each dot represents one mouse ($n = 5$ per group). Representative gene expression in the hippocampus of the 5XFAD mice for **(e)** *Il-1 β* , *Il-6*, *Il-18*, *Ccl12*, **(f)** for *Trem2*. Gene expression levels were determined by real-time PCR. Values in bar graphs are adjusted to 100% for relative gene expression of the WT control. Bars represent mean \pm SEM. Unpaired Student's t-test or one-way ANOVA with Tukey post hoc analysis, * $P < 0.05$; $n = 5-6$ per group. CA: Cornu Amonis; DG: Dentate gyrus.

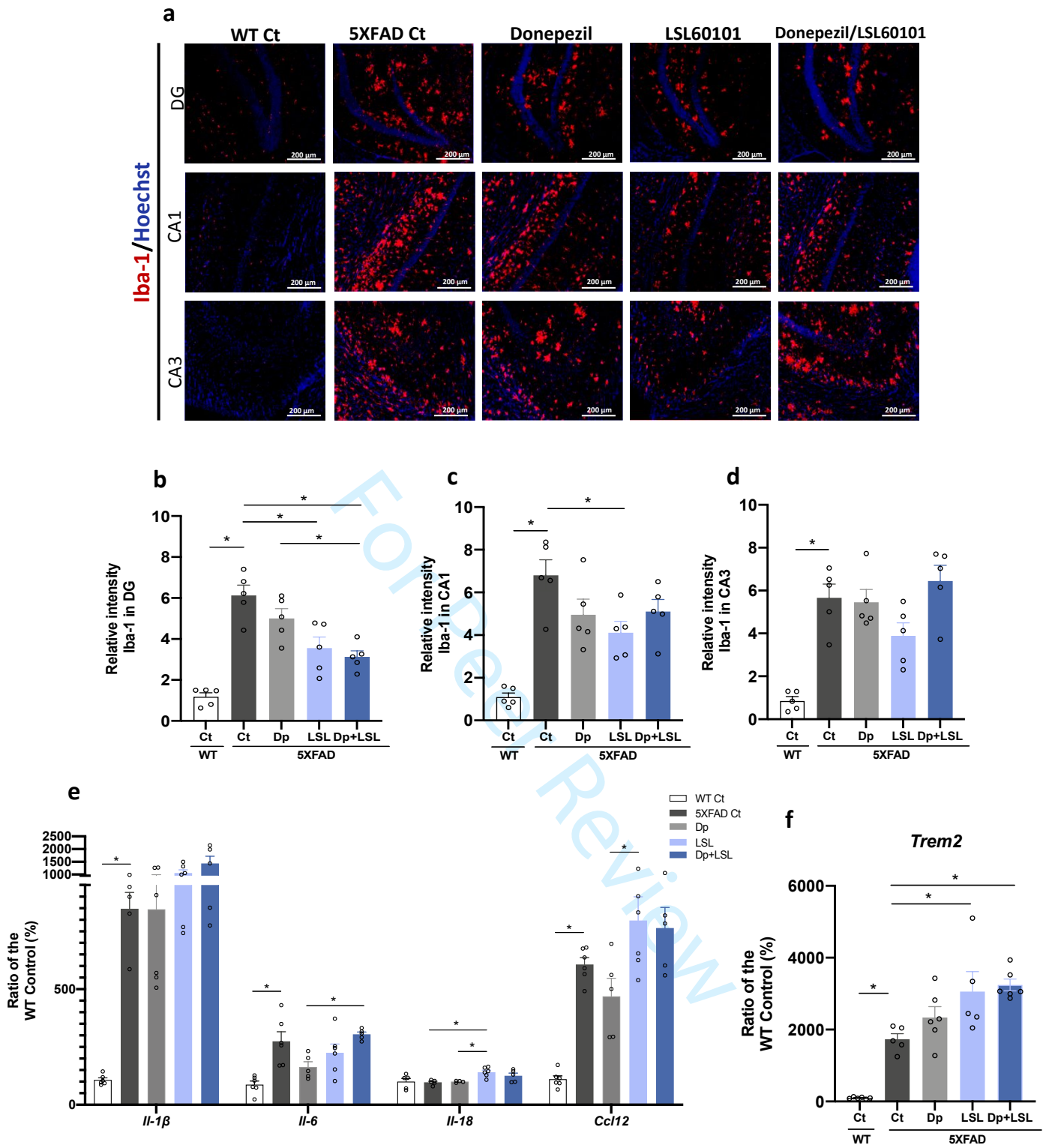
Figure 6. Effects of low dose chronic treatments I2-IR LSL60101, donepezil and co-administration on astrogliosis and synaptic plasticity in 5XFAD mice. **(a)** Representative images of GFAP immunostaining and quantification **(b-d)** in DG, CA1, CA3 areas of the hippocampus of the 5XFAD mice. Data are presented as the mean \pm SEM of relative fluorescent intensity of the positive cells averaged from 2-3 different sections from the same brain area/animal, and each dot represents one mouse ($n = 5$ per group). Representative Western Blot and quantifications **(f-h)** for PSD95 and SYN in the hippocampus of 5XFAD mice. Values in bar graphs are adjusted to 100% for protein levels of the control WT. Bars represent mean \pm SEM. Unpaired Student's t-test or one-way ANOVA with Tukey post hoc analysis, * $P < 0.05$; $n = 5-6$ per group. CA: Cornu Amonis; DG: Dentate gyrus.

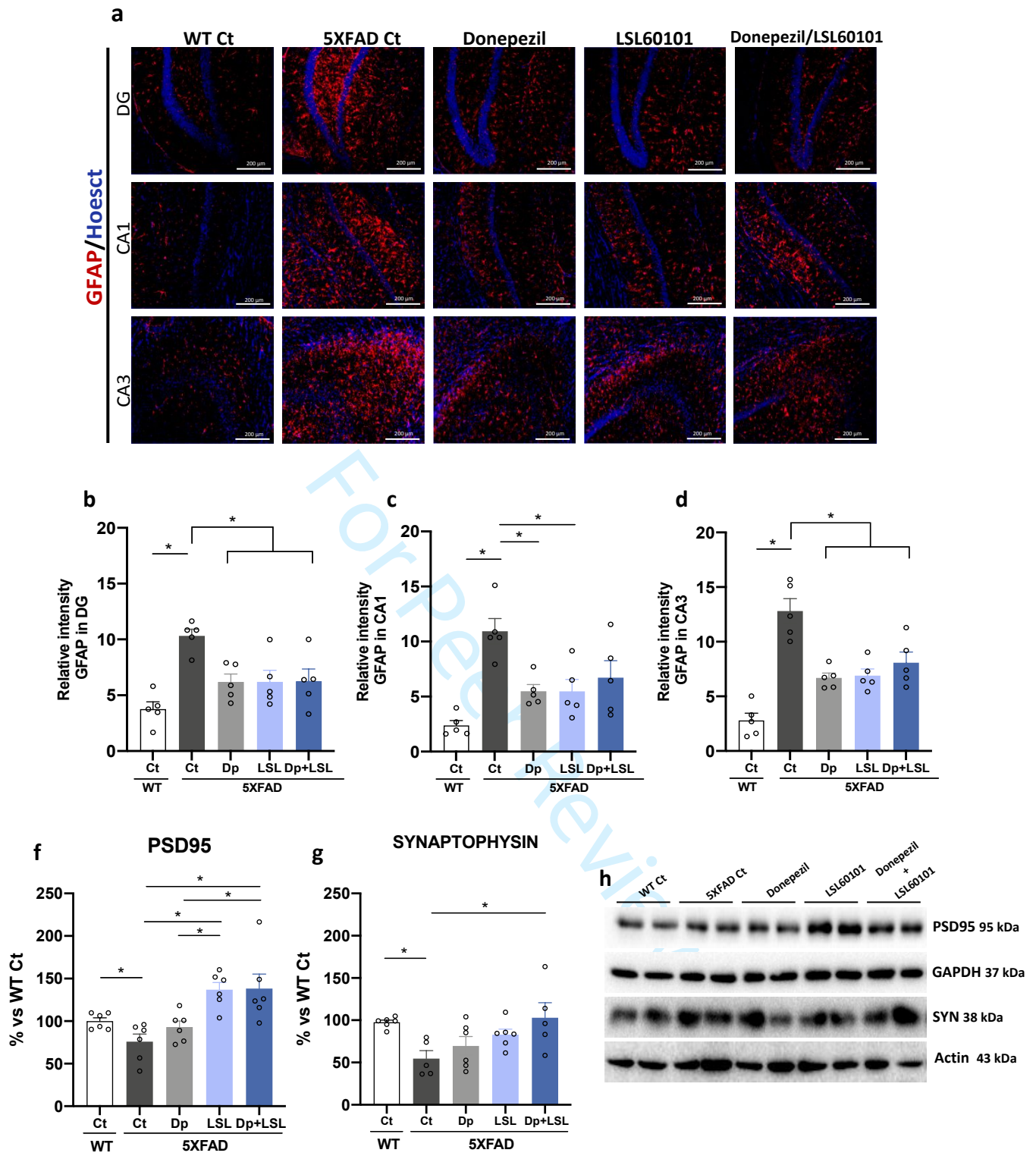












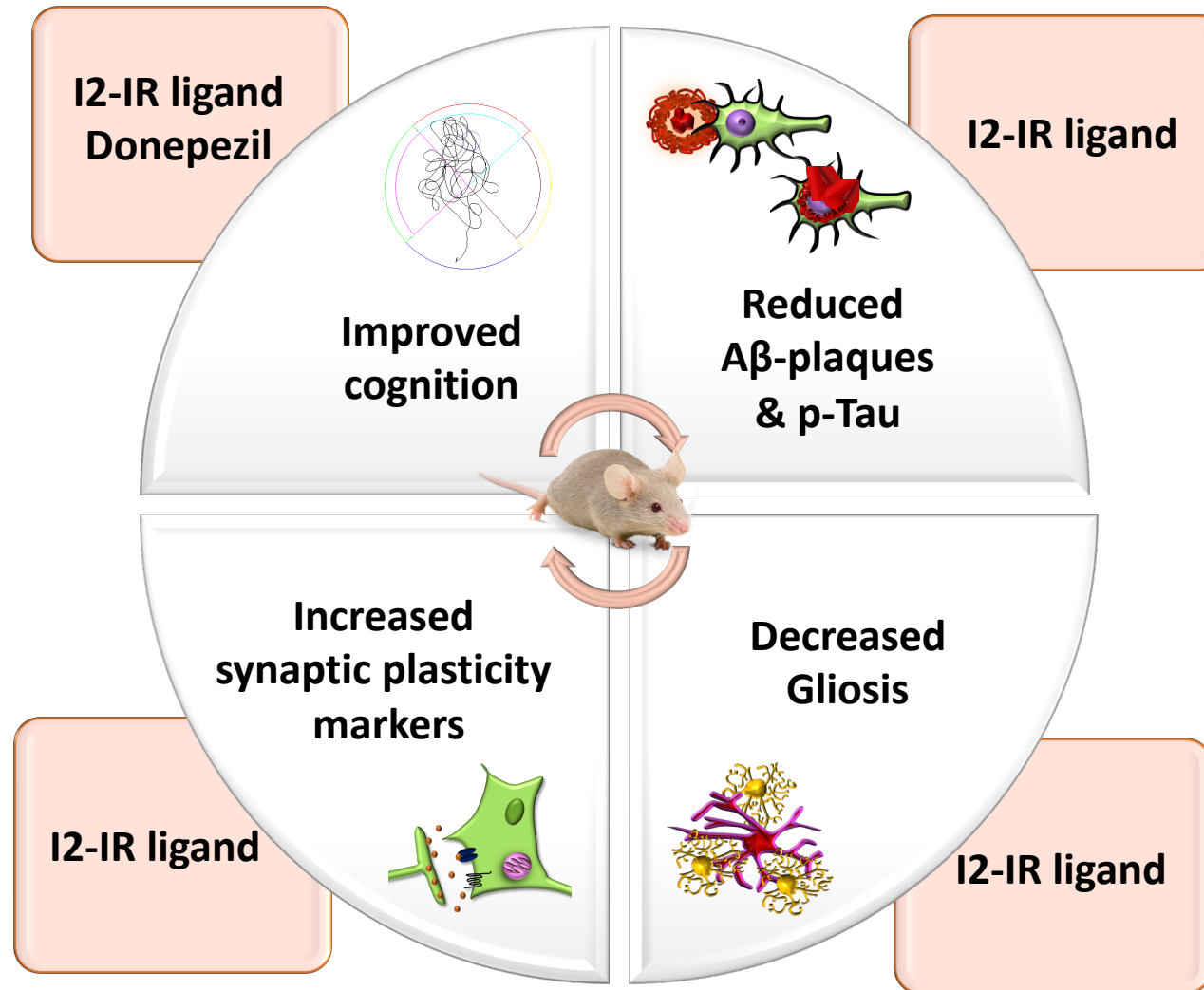


Figure S1: Weekly body weight control during treatment period. Bars represent mean \pm SEM. *Statistics:* One-Way ANOVA with Tukey's Post hoc analysis between weekly controls for each group.

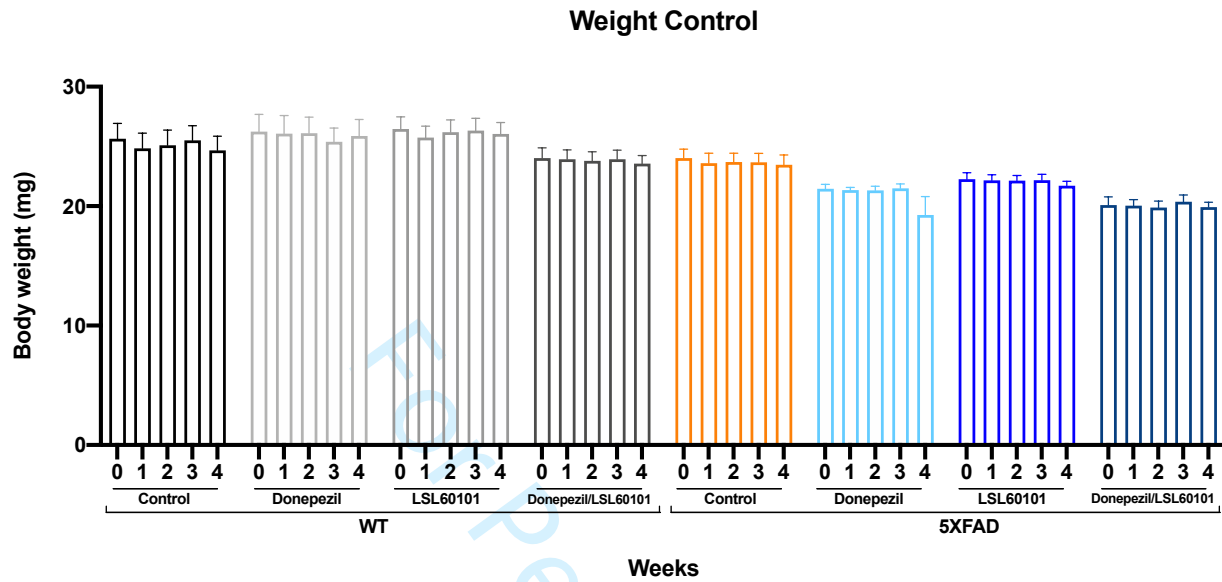


Figure S2. Effects of low-dose chronic treatment with I2-IR LSL60101, Donepezil and co-administration on cognitive status in 5XFAD and WT mice. Results of MWM: (a) Latency to 1st platform quadrant entry (sec) (b) Entries in platform Quadrant (c) Distance to target (cm). Bars represent mean \pm SEM. Two-way ANOVA with Tukey post hoc analysis, * $P < 0.05$; $n = 9-12$ per group; 5XFAD $n = 10-12$ per group

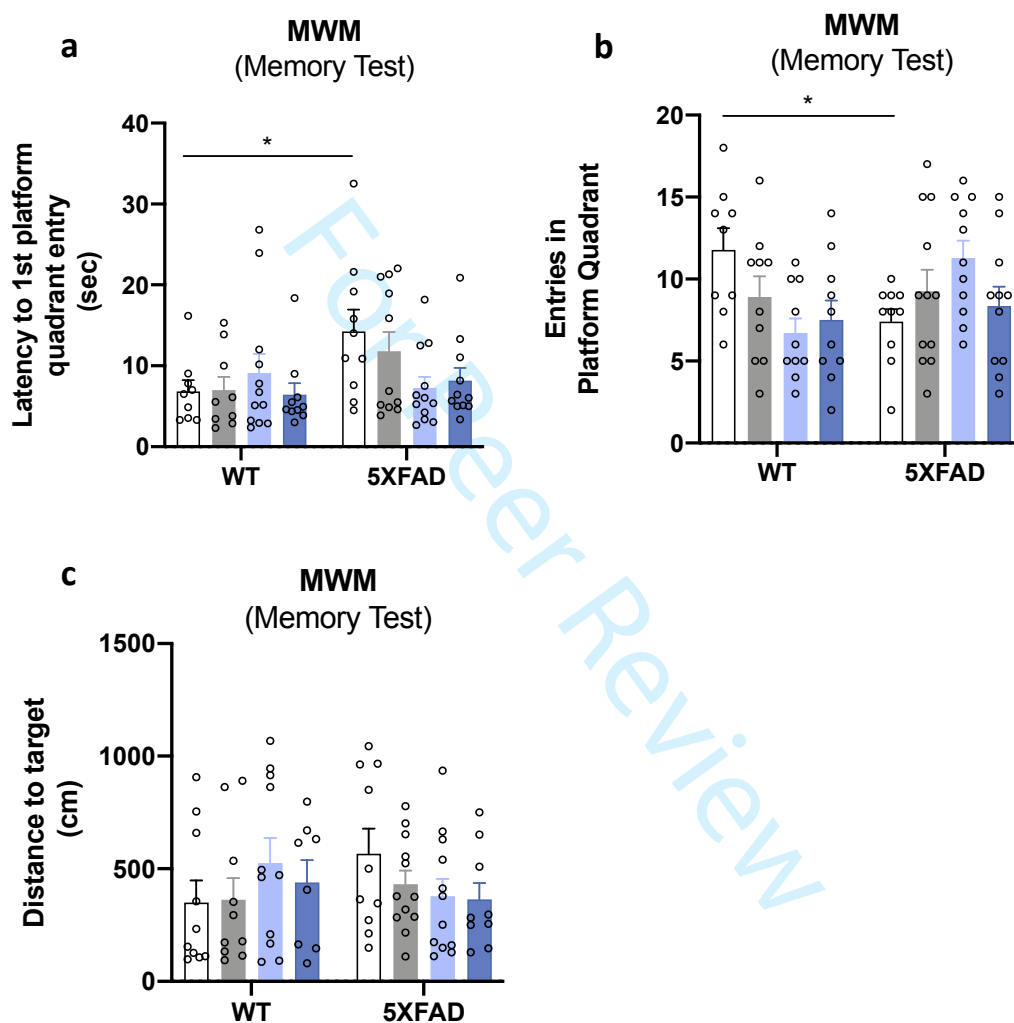


Figure S3: Effects of low dose chronic treatments I2-IR LSL60101, donepezil and co-administration on microgliosis in 5XFAD mice. Representative images and quantification of Iba-1 immunostaining in the cortex (**a-b**). Data are presented as the mean \pm SEM of relative fluorescent intensity of the positive cells averaged from 2-3 different sections from the same brain area/animal and each dot represents one mouse (n=5 per group). Bars represent mean \pm SEM. Unpaired Student's t-test or one-way ANOVA with Tukey post hoc analysis, *P<0.05.

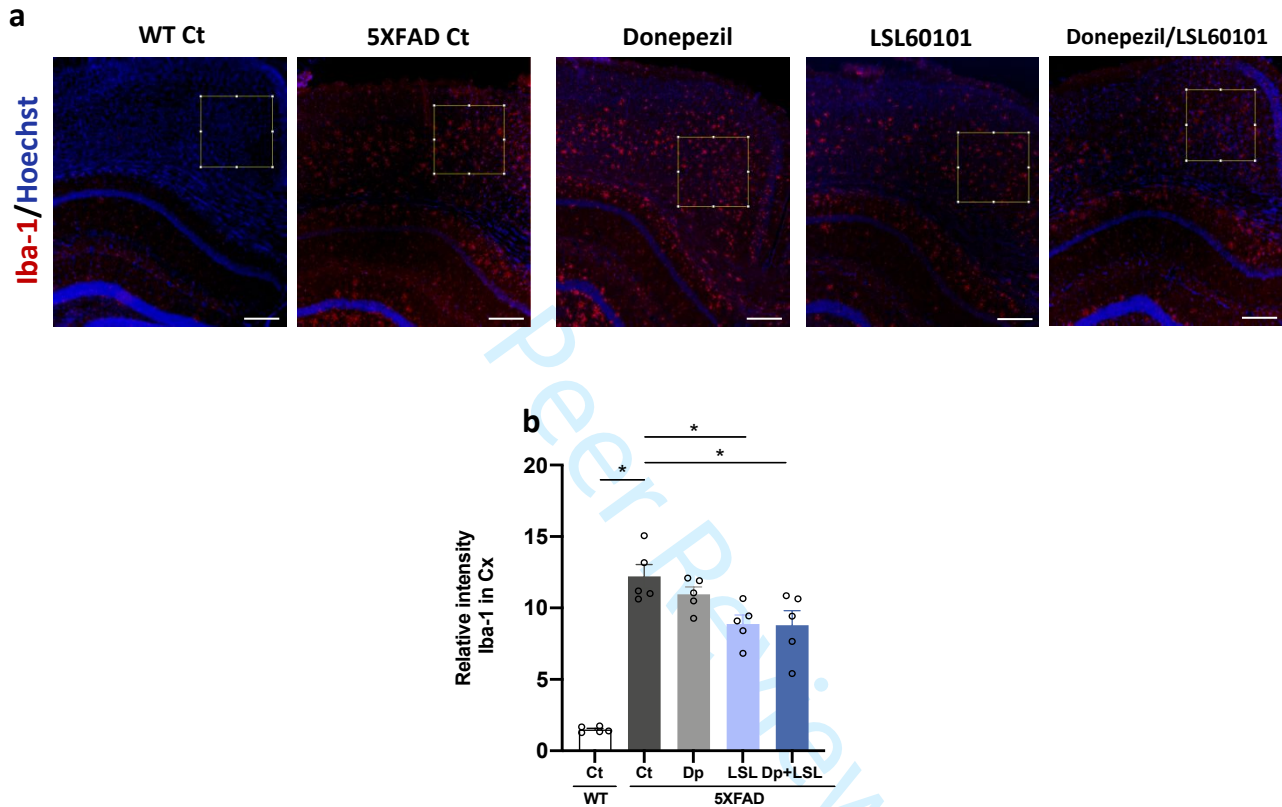


Table S1. Antibodies used in Western Blot (WB) and Immunohistochemistry (IHC)

| Antibody (WB) | Host | Source/Catalog | WB dilution |
|---|-------------|------------------------|---------------------|
| beta Amyloid(H31L21) | Rabbit | Invitrogen/700254 | 1:500 |
| p-Tau (Ser396) | Rabbit | Invitrogen/44752G | 1:1000 |
| p-Tau (Ser404) | Rabbit | Invitrogen/44758G | 1:1000 |
| Tau Total | Mouse | Invitrogen/AHB0042 | 1:1000 |
| APP C-Terminal | Mouse | Covance/SIG-39152 | 1:500 |
| p-APP (T668) | Rabbit | Cell Signaling/3823S | 1:1000 |
| sAPPβ | Rabbit | Covance/SIG-39138-050 | 1:500 |
| sAPPα | Rabbit | Covance/SIG39139 | 1:500 |
| BACE (D10E5) | Rabbit | Cell Signaling/5606 | 1:1000 |
| ADAM10 | Rabbit | Abcam/ab39177 | 1:1000 |
| PSD95 | Rabbit | Abcam/ab18258 | 1:1000 |
| SYN | Mouse | Millipore/MAB5258-20UG | 1:1000 |
| GAPDH | Mouse | Millipore/MAB374 | 1:2500 |
| Actin | Mouse | Invitrogen/MA5-15739 | 1:2500 |
| Goat-anti-mouse HRP conjugated | | Biorad/170-5047 | 1:6000 |
| Goat-anti-rabbit HRP conjugated | | Biorad/170-6515 | 1:6000 |
| Antibody (WB) | Host | Source/Catalog | IHC dilution |
| GFAP (IHC) | Rabbit | Dako/Z0334 | 1:400 |
| IBA-1 (IHC) | Rabbit | Abcam/ab178847 | 1:400 |
| Donkey-anti-rabbit Alexa Fluor 647 | | Invitrogen/ A31573 | 1:500 |

Table S2. Primers and probes used in qPCR studies.

| Target | Product size (bp) | Forward primer (5'-3') | Reverse primer (5'-3') |
|--------------|-------------------|--------------------------------|--------------------------|
| <i>Ide</i> | 287 | CCAAAAGGAAGCGTTCGCC | GGGATCGCTGATGAGAAGCA |
| <i>Nep</i> | 196 | TTGGGAGACCTGGCGGAAAC | CATTCCTTGGACCCTCACCCC |
| <i>Trem2</i> | 269 | CCTGAAGAAGCGGAATGGG | CTTGATTCCTGGAGGTGCT |
| <i>Il-1β</i> | 179 | ACAGAATATCAACCAACAAGTGATATTCTC | GATTCTTTCCTTTGAGGCCCA |
| <i>Il-6</i> | 189 | ATCCAGTTGCCTTCTGGGACTGA | TAAGCCTCCGACTTGTGAAGTGGT |
| <i>Ccl12</i> | 110 | ACACTGGTTCCTGACTCCTCT | ACCTGAGGACTGATGGTGGT |
| <i>Actin</i> | 190 | CAACGAGCGGTCCGAT | GCCACAGGTCCATACCCA |

For Peer Review

Table S4. Parameters measured in the Open Field (OF). (n): number of events. Results are expressed as a mean \pm Standard error of the mean (SEM). Statistics: Two way ANOVA with Tukey post hoc analysis; #p <0.05 vs 5XFAD Control; \$p <0.05 vs 5XFAD LSL60101.

| | WT Control | WT Donepezil | WT LSL60101 | WT Donepezil/LSL60101 | 5XFAD Control | 5XFAD Donepezil | 5XFAD LSL60101 | 5XFAD Donepezil/LSL60101 |
|-----------------------------------|----------------------|----------------------|-----------------------|-----------------------|---------------------|-------------------------|----------------------|--------------------------|
| Total Distance (cm) | 2642,71 \pm 399,64 | 2398,54 \pm 182,64 | 2785,73 \pm 163,37 | 1753,28 \pm 116,27 | 2468,28 \pm 27823 | 2098,37 \pm 194,44 | 2020,04 \pm 117,03 | 2505,23 \pm 150,04 |
| Time spent in Centre (sec) | 7,57 \pm 0,85 | 7,96 \pm 1,22 | 7,09 \pm 1,71 # | 6,14 \pm 1,04 # | 14,92 \pm 3,24 | 6,02 \pm 1,04 #,\$ | 13,67 \pm 2,38 | 5,62 \pm 0,85 #,\$ |
| Time spent in Border (sec) | 245,51 \pm 9,82 | 239,76 \pm 5,40 | 250,45 \pm 4,42 | 264,24 \pm 6,37 | 239,87 \pm 8,11 | 264,89 \pm 3,18 | 247,82 \pm 6,09 | 265,70 \pm 6,32 |
| Distance in Center (%) | 3,24 \pm 0,31 | 3,46 \pm 0,37 | 2,54 \pm 0,34 | 3,03 \pm 0,35 | 3,74 \pm 0,82 | 2,42 \pm 0,26 | 3,65 \pm 0,24 | 1,92 \pm 0,27 #, \$ |
| Distance in Border (%) | 76,92 \pm 2,98 | 74,27 \pm 1,80 | 78,74 \pm 1,59 | 80,83 \pm 2,15 | 76,45 \pm 3,03 | 84,18 \pm 0,97 | 79,19 \pm 1,42 | 82,89 \pm 2,80 |
| Entries in Centre (n) | 11,09 \pm 2,62 | 10,92 \pm 1,59 | 8,36 \pm 1,06 | 5,80 \pm 1,42 | 8,70 \pm 2,07 | 5,17 \pm 0,63 | 7,00 \pm 0,62 | 5,91 \pm 0,62 |
| Rearings (n) | 27,00 \pm 3,47 | 36,82 \pm # | 38,25 \pm 2,72 # | 31,18 \pm 2,85 | 22,90 \pm 3,53 | 28,33 \pm 3,18 | 20,17 \pm 1,26 | 33,58 \pm 2,84 \$ |
| Groomings (n) | 1,09 \pm 0,34 | 1,18 \pm 0,33 | 1,30 \pm 0,39 | 1,73 \pm 0,59 | 1,20 \pm 0,39 | 1,08 \pm 0,33 | 1,42 \pm 0,42 | 1,25 \pm 0,37 |
| Defecations (n) | 1,00 \pm 0,23 | 1,18 \pm 0,40 | 1,42 \pm 0,43 | 1,55 \pm 0,37 | 1,00 \pm 0,39 | 1,08 \pm 0,42 | 1,4 \pm 0,34 | 0,67 \pm 0,22 |
| Urinations (n) | 0,45 \pm 0,21 | 0,55 \pm 0,28 | 0,92 \pm 0,58 | 1,55 \pm 0,55 | 0,70 \pm 0,26 | 0,58 \pm 0,27 | 0,33 \pm 0,19 | 0,08 \pm 0,008 |

Table S4. Parameters measured in the Elevate plus maze (EPM). (n): number of events. Results are expressed as a mean \pm Standard error of the mean (SEM). Statistics: Two way ANOVA with Tukey post hoc analysis; #p <0.05vs 5XFAD Control

| | WT Control | WT Donepezil | WT LSL60101 | WT Donepezil/LSL60101 | 5XFAD Control | 5XFAD Donepezil | 5XFAD LSL60101 | 5XFAD Donepezil/LSL60101 |
|--|-------------------------|-------------------------|-------------------------|-------------------------|--------------------|-------------------------|--------------------|--------------------------|
| Total Distance (cm) | 819,95 \pm 58,32 | 1006,53 \pm 65,23 | 937,28 \pm 50,33 | 759,31 \pm 41,66 | 882,55 \pm 91,52 | 848,33 \pm 62,74 | 858,96 \pm 54,74 | 1027,56 \pm 54,75 |
| Time spent in Open Arms (sec) | 50,79 \pm 12,56 # | 81,71 \pm 9,37 # | 70,28 \pm 10,10 # | 34,25 \pm 4,64 # | 190,06 \pm 12,74 | 115,65 \pm 21,58 # | 171,93 \pm 15,19 | 122,20 \pm 12,19 # |
| Time Spent in Closed Arms (sec) | 188,67 \pm 18,63 # | 132,25 \pm 11,82 # | 166,04 \pm 12,89 # | 197,16 \pm 14,32 # | 57,68 \pm 10,06 | 122,69 \pm 17,06 # | 73,22 \pm 9,63 | 112,16 \pm 12,03 # |
| Distance in Open Arms (%) | 15,51 \pm 3,65 # | 26,61 \pm 2,10 # | 21,74 \pm 3,11 # | 15,62 \pm 2,42 # | 53,12 \pm 4,06 | 34,28 \pm 6,41 # | 48,81 \pm 4,20 | 40,27 \pm 4,29 |
| Distance in Closed Arms (%) | 66,78 \pm 4,55 # | 53,58 \pm 2,39 # | 60,52 \pm 3,69 # | 68,13 \pm 3,39 # | 28,79 \pm 3,77 | 47,19 \pm 5,23 # | 34,53 \pm 3,54 | 46,51 \pm 3,32 # |
| Rearings (n) | 13,55 \pm 1,51 # | 15,50 \pm 1,76 # | 13,92 \pm 1,25 # | 14,82 \pm 1,21 # | 5,70 \pm 1,18 | 12,45 \pm 1,19 # | 8,83 \pm 1,56 | 13,83 \pm 1,59 # |
| Groomings (n) | 1,36 \pm 0,15 | 1,33 \pm 0,26 | 1,91 \pm 0,16 | 2,09 \pm 0,31 | 1,50 \pm 0,22 | 1,08 \pm 0,15 | 1,09 \pm 0,24 | 1,30 \pm 0,14 |
| Defecations (n) | 1,45 \pm 0,45 | 1,27 \pm 0,48 | 0,83 \pm 0,39 | 1,27 \pm 0,33 | 0,55 \pm 0,27 | 0,25 \pm 0,13 | 0,75 \pm 0,22 | 1,33 \pm 0,33 |
| Urinations (n) | 0,64 \pm 0,24 | 0,33 \pm 0,19 | 0,25 \pm 0,13 | 0,30 \pm 0,15 | 0,00 \pm 0,00 | 0,25 \pm 0,13 | 0,08 \pm 0,08 | 0,00 \pm 0,00 |